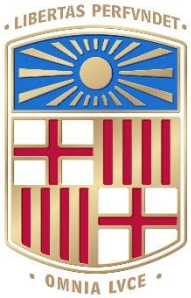

UNIVERSITAT DE BARCELONA

Final Degree Project

Biomedical Engineering Degree

FETAL HEART COMPUTATIONAL MODELING

Barcelona, 21 January 2022

Author: Laura Gargallo Ferrer

Director: Patricia Garcia Cañadilla

Tutor: Fàtima Crispi Brillas

ACKNOWLEDGEMENTS

I would like to express my sincere gratitude to my director, Dr. Patricia Garcia, for teaching me and supervising my final degree project, and helping and guiding me during the whole project development. Without her constant support and her critical feedback and suggestions, I would not have been able to complete this project. Further, I would also like to thank my tutor, Dr. Fàtima Crispi, for giving me the opportunity to do this stimulating project in the BCNatal research group.

Moreover, I must thank my parents, sisters and friends for giving me the necessary support during all the years of university, but specially, during these last months for encouraging me to carry on this project.

ABSTRACT

Among infants born with cardiac defects, congenital heart disease (CHD) is the leading congenital abnormality and it origins the majority of newborns death in developed countries. The structural malformations in the heart or great vessels it causes increase the postnatal cardiovascular risk and mortality. In particular, the high incidence of tetralogy of Fallot (ToF) in live births make essential to develop new procedures that enable the study and understanding of this cardiac disorder and the hemodynamic changes it induces. That way, fetal medicine has been constantly evolving in the past years, and computational modeling techniques are becoming more established in the clinical practice and are of growing importance. Nowadays, different 0D lumped parameters models have demonstrated to be useful to evaluate complex cardiac defects in order to aid health workers and find the best management for patients.

In this project, a 0D lumped model simulating hemodynamic components and parameters of the fetal heart was developed to study the changes occurring in a ToF heart. Specifically, birth defects of ventricular septal defect (VSD) and pulmonary valve stenosis (PVS) were modeled, allowing the analysis of their effects in fetal circulation.

Our results suggested that the designed 0D lumped model can reproduce the blood velocities and pressure waveforms of the fetal heart in healthy conditions after adjusting the values of some model parameters. Despite that, the parameters of the ductus arteriosus (DA) should be better fit since we could not completely reproduce its velocity waveform. Regarding the evaluation of hemodynamic changes of cardiac defects, results suggested that the 0D lumped model can simulate the features present in ToF, such as the right-to-left shunt, characteristic of blood flow in VSD, and the increase of the pressure gradient and peak velocity of the pulmonary artery, indicative of PVS. However, more literature and clinical data of cardiac defects should be used in order to verify these outcomes and ensure their reliability.

Keywords: 0D lumped parameter model / Fetal heart / Hemodynamics / Tetralogy of Fallot / Ventricular septal defect / Pulmonary valve stenosis.

TABLE OF CONTENTS

LIST OF FIGURES ..... **VII**

LIST OF TABLES ..... **X**

LIST OF ABBREVIATIONS ..... **XI**

1) INTRODUCTION **1**

1.1) DESCRIPTION OF THE PROJECT 1

1.2) OBJECTIVES 2

1.3) METHODOLOGY 2

1.4) SCOPE AND SPAN OF THE PROJECT 3

2) BACKGROUND **5**

2.1) STATE-OF-THE-ART 5

2.1.1) Congenital heart diseases *5*

2.1.2) Computational models of the fetal circulation *7*

2.2) STATE OF THE SITUATION 10

3) MARKET ANALYSIS **13**

3.1) SECTORS TO WHICH IT IS ADDRESSED 13

3.2) HISTORICAL EVOLUTION OF THE MARKET 13

3.3) FUTURE MARKET PROSPECTS 14

4) CONCEPTION ENGINEERING **16**

4.1) STUDY INDIVIDUALS 16

4.2) PROPOSED SOLUTION 17

4.3) ALTERNATIVE SOLUTIONS 18

5) DETAILED ENGINEERING **20**

5.1) INPUT DATA 20

5.2) FETAL HEART 0D LUMPED PARAMETER MODEL WITH AND WITHOUT CARDIAC DEFECTS 21

5.2.1) Ventricles of the heart *22*

5.2.2) Aortic and pulmonary valves *23*

5.2.3) Systemic and pulmonary circulations ... *24*

5.2.4) Fetal heart model with VSD and PVS ... *25*

5.3) PARAMETRIC ANALYSIS IN HEALTHY CONDITIONS ... 26

5.4) CALIBRATION OF THE SIMPLIFIED MODEL OF THE FETAL HEART IN HEALTHY CONDITIONS ... 27

5.5) PARAMETRIC ANALYSIS OF THE FETAL HEART MODEL WITH VSD AND PVS ... 28

6) RESULTS AND DISCUSSION ... 29

6.1) PARAMETRIC ANALYSIS IN HEALTHY CONDITIONS ... 29

6.1.1) Peripheral resistances and compliances of pulmonary and systemic vascular beds ... *29*

6.1.2) Ventricular activation timings ... *30*

6.1.3) Diameters of mitral and tricuspid valves ... *31*

6.2) CALIBRATION OF THE SIMPLIFIED MODEL OF THE FETAL HEART IN HEALTHY CONDITIONS ... 32

6.3) EVALUATION OF HEMODYNAMIC CHANGES OF CARDIAC DEFECTS IN FETAL CIRCULATION ... 34

6.3.1) VSD size ... *34*

6.3.2) PVS degree ... *35*

7) EXECUTION SCHEDULE ... 38

7.1) TASKS AND TIME DEFINITION – WBS ... 38

7.1.1) Bibliographic research ... *38*

7.1.2) Fetal heart model development and implementation ... *39*

7.1.3) Parametric analysis of model parameters ... *40*

7.1.4) Fetal heart model calibration and validation ... *40*

7.1.5) Evaluation of hemodynamic changes in cardiac defects ... *40*

7.1.6) Writing of the project report ... *41*

7.2) TIMING. PHASES AND MILESTONES – GANTT DIAGRAM ... 41

8) TECHNICAL VIABILITY ... 43

8.1) SWOT ANALYSIS ... 43

9) ECONOMIC VIABILITY ... 44

9.1) ESTIMATION AND ANALYSIS OF COSTS AND BUDGETS ... 44

10) REGULATORY AND LEGAL ASPECTS 46

10.1) APPLICABLE LAW: NORMS AND REGULATIONS 46

11) CONCLUSIONS AND FUTURE LINES 47

BIBLIOGRAPHY 49

APPENDIX 54

APPENDIX A – PARAMETRIC ANALYSIS IN HEALTHY CONDITIONS 54

Peripheral resistances and compliances of pulmonary and systemic vascular beds 54

APPENDIX B – PARAMETRIC ANALYSIS IN HEALTHY CONDITIONS 57

Ventricular activation timings 57

APPENDIX C – PARAMETRIC ANALYSIS IN HEALTHY CONDITIONS 59

Diameters of mitral and tricuspid valves 59

APPENDIX D – CALIBRATION OF THE SIMPLIFIED MODEL OF THE FETAL HEART IN HEALTHY CONDITIONS 60

LIST OF FIGURES

Figure 1. Flowchart of the project methodology 3

Figure 2. Classical ToF anatomy and its birth defects: (1) overriding aorta, (2) pulmonary infundibular stenosis, (3) ventricular septal defect, (4) right ventricular hypertrophy. (Ao: aorta, LA: left atrium, LV: left ventricle, PA: pulmonary artery, RA: right atrium, RV: right ventricle) [14] 6

Figure 3. Diagram of the different types of ToF and its pathophysiologic effects [13] 7

Figure 4. Analogy between the fire engine with the Windkessel and the arterial system 8

Figure 5. Models that describe the different components of the CVS. a) 3-element WK model – Modification from [26], b) L-element model [27], c) Model of the ventricle and arterial valve – Modification from [28] 10

Figure 6. Fetal circulation model: a) Anatomical simplified configuration, and b) Equivalent electrical lumped model 11

Figure 7. Mitral biphasic inflow (E and A waveforms) and aortic outflow (Ao waveform) in a spectral Doppler image. Time intervals include: IVCT, ET, and IVRT – Modification from [51] 17

Figure 8. Computed atrial input velocity, from left and right atria, respectively 21

Figure 9. 0D lumped model of a normal fetal heart. a) Anatomical configuration of the model, b) Equivalent electric circuit (LA: left atrium, LV: left ventricle, RA: right atrium, RV: right ventricle, aV: aortic valve, pV: pulmonary valve, aAo: ascending aorta, tAo: thoracic aorta, pA: main pulmonary artery, lpA: left pulmonary artery, rpA: right pulmonary artery, QmV: mitral valve flow, QtV: tricuspid valve flow, U: isovolumic pressure generator, E: elastance, s: systemic vasculature, LL: left lung, RL: right lung, DA/duct: ductus arteriosus) 21

Figure 10. a) Activation function of the fetal ventricles; b) Time-varying elastance of the fetal ventricles 23

Figure 11. Equivalent electric circuit of a fetal heart with VSD. (QmV: mitral valve flow, QtV: tricuspid valve flow, U: isovolumic pressure generator, E: elastance, LV: left ventricle, RV: right ventricle, aV: aortic valve, pV: pulmonary valve, aAo: ascending aorta, tAo: thoracic aorta, s: systemic vasculature, pA: main pulmonary artery, lpA: left pulmonary artery, rpA: right pulmonary artery, LL: left lung, RL: right lung, DA/duct: ductus arteriosus) 25

Figure 12. Model-based waveforms resulting from the parametric study on the variation of the peripheral compliance of the pulmonary circulation vascular bed ($Clungs$): a) left ventricle and aorta pressure; b) right ventricle and pulmonary artery pressure; c) aorta velocity; d) pulmonary artery velocity; e) DA velocity 29

Figure 13. Model-based ventricular activation waveform resulting from the parametric study on the variation of: a) ventricular contraction duration (Tv); b) delay between atrial and ventricular contraction ($delay$) 30

Figure 14. Model-based waveforms resulting from the parametric study on the variation of the mitral valve diameter: a) left ventricle and aorta pressure; b) right ventricle and pulmonary artery pressure; c) aorta velocity; d) pulmonary artery velocity; e) DA velocity 31

Figure 15. Model-based pressure waveforms of a) left ventricle and aorta, and b) right ventricle and pulmonary artery; after calibration of the fetal heart 0D lumped model 32

Figure 16. Measured and model-based velocity profiles of a) aortic valve, b) main pulmonary valve, and c) DA; after calibration of the fetal heart 0D lumped model 33

Figure 17. Model-based velocity profiles of mitral and aortic valves, highlighting the different cardiac events of mitral and aortic valves opening/closing, which designate the four cardiac timings (from left to right): FT, IVCT, ET, IVRT (MV: mitral valve, AV: aortic valve)..... 33

Figure 18. Model-based blood flow in a) left and b) right ventricles; when there is VSD in the fetal heart..... 34

Figure 19. Model-based pressure in a) left and b) right ventricles; when there is VSD in the fetal heart..... 35

Figure 20. Model-based velocity profile in the pulmonary artery when there is PVS in the fetal heart..... 36

Figure 21. Model-based pressure when there is PVS in the fetal heart in: a) Right ventricle, b) Pulmonary artery..... 36

Figure 22. Model-based waveforms in the right ventricle when there is PVS in the fetal heart: a) Ventricular pressure-volume relationship, b) Ventricle blood flow (RV: right ventricle) 37

Figure 23. WBS of the project development..... 38

Figure 24. Gantt diagram of the final degree project..... 42

Figure A1. Model-based waveforms resulting from the parametric study on the variation of the peripheral compliance of the systemic circulation vascular bed (Cs): a) left ventricle and aorta pressure; b) right ventricle and pulmonary artery pressure; c) aorta velocity; d) pulmonary artery velocity; e) DA velocity..... 54

Figure A2. Model-based waveforms resulting from the parametric study on the variation of the peripheral resistance of the pulmonary circulation vascular bed (Rlungs): a) left ventricle and aorta pressure; b) right ventricle and pulmonary artery pressure; c) aorta velocity; d) pulmonary artery velocity; e) DA velocity..... 55

Figure A3. Model-based waveforms resulting from the parametric study on the variation of the peripheral resistance of the systemic circulation vascular bed (Rs): a) left ventricle and aorta pressure; b) right ventricle and pulmonary artery pressure; c) aorta velocity; d) pulmonary artery velocity; e) DA velocity..... 56

Figure B1. Model-based elastance waveform resulting from the parametric study on the variation of: a) ventricular contraction duration (Tv); b) delay between atrial and ventricular contraction (delay) 57

Figure B2. Model-based waveforms resulting from the parametric study on the variation of the ventricular contraction duration (Tv): a) left ventricle and aorta pressure; b) right ventricle and pulmonary artery pressure; c) aorta velocity; d) pulmonary artery velocity; e) DA velocity 57

Figure B3. Model-based waveforms resulting from the parametric study on the variation of the delay between atrial and ventricular contraction (delay): a) left ventricle and aorta pressure; b)

right ventricle and pulmonary artery pressure; c) aorta velocity; d) pulmonary artery velocity; e) DA velocity 58

Figure C1. Model-based waveforms resulting from the parametric study on the variation of the tricuspid valve diameter: a) left ventricle and aorta pressure; b) right ventricle and pulmonary artery pressure; c) aorta velocity; d) pulmonary artery velocity; e) DA velocity 59

Figure D1. Model-based blood flow in a) left and b) right ventricles, after calibration of the fetal heart 0D lumped model 60

Figure D2. Model-based pressure-volume relationship of a) left and b) right ventricles, after calibration of the fetal heart 0D lumped model 60

Figure D3. Model-based velocity profile of aortic (solid line) and pulmonary (dashed line) valves, after calibration of the fetal heart 0D lumped model 61

Figure D4. Model-based blood velocity profiles of the pulmonary circulatory system: a) left and b) right lungs, after calibration of the fetal heart 0D lumped model 61

LIST OF TABLES

Table 1. Variables that characterize the hydraulic network and their electrical analogues..... 8

Table 2. Comparison of modeling techniques in time domain for the study of cardiovascular dynamics..... 19

Table 3. Specific clinical data of a patient from Hospital Clínic de Barcelona (EFW: estimated fetal weight, GA: gestational age, FT: filling time, IVCT: isovolumic contraction time, ET: ejection time, IVRT: isovolumic relaxation time, T_c: total cycle duration, HR: heart beat, E: early or passive diastole, A: atrial, active or late diastole)..... 20

Table 4. Parameter values used in the fetal heart model of this project..... 24

Table 5. Equations describing the vessel's physical dimensions (length, diameter and E: Young's modulus) as a function of gestational age in weeks for the 6 arterial segments included in the final lumped model 24

Table 6. Initial values of peripheral resistances and compliances..... 25

Table 7. Minimum and maximum values for peripheral resistances and compliances, ventricular systolic time and time delay between atrial and ventricular systole, and diameters of atrioventricular valves 26

Table 8. Grading of PVS severity..... 28

Table 9. Initial and final values after calibration of the fetal heart 0D lumped model..... 32

Table 10. Measured and modeled values after calibration of the fetal heart 0D lumped model, and its relative error 33

Table 11. Pressure gradient across the pulmonary valve when there is PVS in the fetal heart ... 35

Table 12. Summary of the total amount of hours required for the project development..... 41

Table 13. SWOT analysis of the project..... 43

Table 14. Summary of total costs of this final degree project..... 45

LIST OF ABBREVIATIONS

0D lumped model – Zero-dimensional lumped model

CHD – Congenital Heart Disease

CVS – Cardiovascular System

DA – Ductus Arteriosus

DBP – Diastolic Blood Pressure

EFW – Estimated Fetal Weight

ET – Ejection Time

FT – Filling Time

GA – Gestational Age

HR – Heart Rate

IUGR - Intrauterine Growth Restriction

IVCT – Isovolumic Contraction Time

IVRT – Isovolumic Relaxation Time

MBP – Mean Blood Pressure

ODE – Ordinary Differential Equation

PVS – Pulmonary Valve Stenosis

RVH – Right Ventricular Hypertrophy

RVOTO – Right Ventricular Outflow Tract Obstruction

SBP – Systolic Blood Pressure

ToF – Tetralogy of Fallot

VSD – Ventricular Septal Defect

WK – Windkessel

1) INTRODUCTION

The purpose of this first section is to introduce an overview of the Final Degree Project *Fetal heart computational modeling*. Along this section, there is going to be defined the detailed description of the project development, its outlined objectives, the designed methodology that has been followed and, finally, a definition of the scope and content of the study.

1.1) Description of the project

Cardiac mathematical modeling and simulation techniques are becoming more and more important because they enable to better understand the overall cardiovascular system (CVS), the mechanisms of circulatory physiology and the complex interconnections between the heart chambers, blood vessels and blood constituents. These relationships can be translated into mathematical formulas (i.e., differential equations), which are established by different laws of conservation, such as mass, momentum and charge conservation laws, and which are employed to quantify different biomechanical conditions [1]. In that way, *in silico* models of the CVS are valuable for the comprehension of the causes and defects of cardiac disorders, as well as for the personalization of predictive medicine, which, at the end, accounts for an optimization of the treatment so that there is the best prospective response possible, and the medical care is beneficial [2].

There is a wide range of cardiovascular modeling techniques in order to study and comprehend the mechanism of hemodynamics, both in healthy and pathological conditions. As it is going to be described in the next sections, this project is focused on a zero-dimensional (0D) lumped parameter model which is characterized by having a uniform distribution of the fundamental variables, such as blood pressure, flow and volume, in space and time. This is translated into a simplification of the different components of the CVS by means of the existing hydraulic-electrical analogy, so blood flow hemodynamics in the circulatory system can be represented by a set of resistances, capacitances and inductances. This is a widely used method for cardiovascular simulations in order to study the hemodynamics in patients [3].

Congenital heart disease (CHD) is the most frequent congenital disorder that newborns suffer, with an approximated birth prevalence of 8 cases per 1000 live births worldwide [4] and accounting for up to 25% of all congenital malformations [5]. It is also the leading cause of infant death from birth defects [4-6]. It accounts for structural abnormalities of the fetal heart and/or great vessels that influence the way they work and the way the blood flows through them, which can result in an increased postnatal cardiovascular risk. Fortunately, fetal cardiovascular medicine and surgery has notably advanced in the past years, prolonging life expectancy in patients suffering from these disorders [6].

Taking this into account, computational models of CHDs have demonstrated to own a fundamental role in the translation of bioengineering into clinics, as they are useful to study their characteristic and complex defects and, consequently, to aid the healthcare personnel in finding the best treatment and surgery planning for improving cardiovascular prognosis. Thus,

mathematical modeling has already been employed for different CHDs, such as patients with single ventricle, transposition of the great arteries and aortic coarctation, among others [7-10].

This project has mainly focused on the development of a 0D lumped model of the fetal heart. It has been first calibrated in healthy conditions. Then, new components have been added to the fetal heart model in order to simulate some of the defects present in Tetralogy of Fallot (ToF). These are ventricular septal defect (VSD) and pulmonary valve stenosis (PVS), in order to simulate the blood flow changes in a ToF heart.

1.2) Objectives

The aim of this final degree project is to implement a 0D lumped model of the fetal heart in order to extend a previous 0D lumped model of the fetal vascular circulation and enable the study of different abnormalities in the fetal heart. It is an important step in cardiovascular modeling since there are many CHDs leading to different and complex blood flow changes. Therefore, a better understanding of this is required to improve the prenatal diagnosis and prognosis of CHDs. This enhancement would, consequently, generate a better medical care and treatment. Once properly validated, the resulting 0D lumped model could help the clinicians in the diagnosis and prognosis of CHDs, thus leading to a personalized, non-invasive, fast and efficient medicine, and contribute to the translation of mathematical modeling into clinical practice.

Besides specifying the main goal of the project, which consists in the development of an *in silico* 0D lumped model of the fetal heart, the different specific objectives of this project are defined as follows:

1. Research and analyze the current state-of-the-art of cardiovascular computational modeling, focusing specifically on the fetal heart.
2. Implement a 0D lumped parameter model of the fetal heart in healthy conditions.
3. Extend the fetal heart model by integrating the vascular circulatory system.
4. Perform a parametric study of the different model parameters.
5. Calibrate the developed model by personalizing it with real data from a healthy fetus.
6. Incorporate two of the birth defects present in ToF into the computational model: VSD and PVS.
7. Perform a parametric study to evaluate the changes in hemodynamics due to VSD and PVS.

1.3) Methodology

This final degree project has been carried out from January 2021 to January 2022, thus consisting of one year approximately, under the supervision of Dr. Patricia Garcia Cañadilla. It has been divided in different stages in order to have a practical structure and successfully achieve the main goal of the project. The flowchart of the followed methodology is shown in *Figure 1*, followed by a brief explanation of each one of the stages.

The study has been carried out using Simulink tool, integrated in MATLAB environment (2019b, The MathWorks Inc., Natick, MA), which has enabled the creation of the electrical analog circuit.

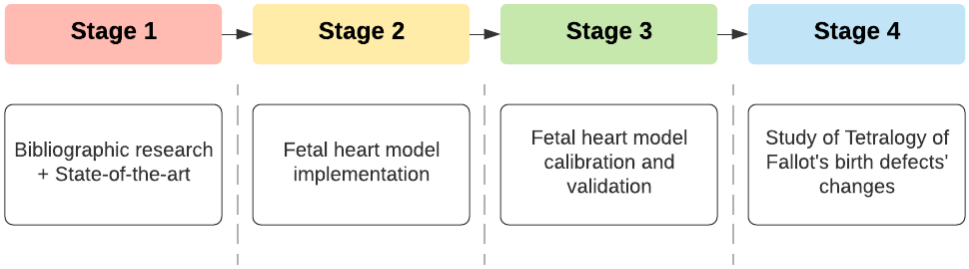

Figure 1. Flowchart of the project methodology

Stage 1. Bibliographic research and review of the state-of-the-art of the already existent computational models of the fetal heart. This will be helpful to get familiarized with the cardiovascular lumped parameter modeling.

Stage 2. Development and implementation of the model of the fetal heart in Simulink, MATLAB. Definition of the electric components, input variables and circuit parameters.

Stage 3. Calibration and validation of the fetal heart model by comparing the simulated outputs with measured data from healthy patients.

Stage 4. Study of the consequences caused by the birth defects of ToF over the fetus hemodynamics (blood flow, pressure and volume).

1.4) Scope and span of the project

This project is aimed at the development and validation of a 0D lumped computational model of the fetal heart. The final goal is to enable the study of the hemodynamics' changes occurring in CHDs, particularly in ToF.

The scope of the project included different topics. Firstly, a deep bibliographic research of fetal heart computational models was done, covering the electrical components and parameters required. Consequently, the 0D lumped model of a normal fetal heart was implemented, which was later modified by adding the vascular circulatory system. Once the model was designed and implemented, parametric studies were performed to study the relative contribution of each individual model parameter into the whole model behavior. Following that, the final estimation of the parameters' values for a fetus in healthy conditions was achieved using an optimization algorithm that minimizes the relative error between the computed and the measured data, meaning that the simulated blood flows can reproduce the real blood flow as accurate as possible. Finally, after having the heart model calibrated, the changes in hemodynamics as a consequence of some of the defects present in ToF were simulated by adding components or changing variables in the original model.

Concerning the span of the project, this has been developed in BCNatal Fetal Medicine Research Center (FMRC) (https://bcnatalresearch.org) and Institut d'Investigacions Biomèdiques August Pi

i Sunyer (IDIBAPS) (https://idibaps.org) at Hospital Clínic and Hospital Sant Joan de Déu. BCNatal-FMRC is a research center that gathers an interdisciplinary research team of more than 100 members, which includes doctors, bioengineers, biologists, pharmacists, epidemiologists and statisticians, all of them focused on providing solutions to fetal and perinatal diseases. It is a recognized university center in maternofetal and neonatal medicine in Europe, and a worldwide reference in this field. With regard to the mission of the center, the main goal is the demonstration of the impact that fetal life has on the future health of children, and it is achieved by developing innovative methods of diagnosis and treatment of prenatal diseases in order to improve the cardiovascular prognosis. Hence, these therapies can be integrated through the Maternal-Fetal Medicine and Neonatology services. Conversely, IDIBAPS is the leading biomedical research center in Spain that strives for excellence in biomedical research to improve people's health and ensure the translational research. It addresses different research areas, such as Translational Computing in Cardiology, a research group focused on assessing cardiac function and understanding changes induced by diseases.

COVID-19 pandemic has forced the final degree project to be entirely performed remotely, and all the meetings with the director and tutor have had to be online as well. The project has been performed with the help of periodic meetings with Dr. Patricia Garcia Cañadilla, a postdoctoral researcher working on the implementation of computational models of the fetal cardiovascular system and synchrotron biomedical imaging, and Dr. Fàtima Crispi, the scientific coordinator of BCNatal-FMRC and coordinator of its Fetal Programming line.

2) BACKGROUND

This section is destined to describe the background of the project. Different scientific publications that describe the current state-of-the-art of computational modeling medicine are mentioned an analyzed, as well as their application into the maternofetal medicine and CHDs. There is also a thorough exposition of the present situation of the fetal circulatory *in silico* model taking into account the previous studies performed by BCNatal research group.

2.1) State-of-the-art

2.1.1) Congenital heart diseases

As it has been previously stated, CHD is the most common congenital disorder occurring in newborns and the first cause of infant mortality from birth defects. It is characterized by developing a serious structural anomaly or malformation in the heart or great vessels during fetal development, which causes a malfunction of the whole circulatory system [4-6]. In Spain, the number of deaths in infants aged less than 1 year that are diagnosed of CHD is 6.23 per 10.000 live births, which represents a 18% of the total infant mortality rate [11]. The causes of CHDs are unknown, and approximately 85% of patients do not have a defined origin. Moreover, although it has been shown that different genetic and environmental factors can influence the appearance of CHD in patients, there is not much information in order to make a clear determination about the risk factors [1]. In that way, it is important to develop new therapies for patients suffering from any CHD to make beneficial follow-up procedures and continue improving the management of the possible complications [12].

There are various types of CHDs that are characterized by different birth defects. This project is focused on one of these CHDs: ToF. It is one of the most frequent CHDs, representing about 7-10% of all of them, with an incidence of 1 in 3.500 live births (2019) [13]. As its name indicates, it consists of a rare combination of four defects: VSD, PVS, hypertrophy of the right ventricle, and an overriding aorta. These major features are depicted in *Figure 2* [14].

1) *VSD*

VSD is an abnormal hole in the ventricular septum, which is the wall between the two ventricles of the heart, particularly located in its perimembranous and muscular regions. It allows the blood to flow between these two chambers, usually from the right side to the left one (right-to-left shunt), which produces cyanosis in the early postnatal period, a disorder that consists in shunting poorly oxygenated blood into the systemic circulation, and that generates bluish discoloration of the skin and mucous membranes [14].

2) *PVS – Right ventricular outflow tract obstruction (RVOTO)*

This condition is characterized by the reduction of the pulmonary valve, which causes an obstruction to pulmonary blood flow at the level of the right ventricle outflow tract [13]. There are different variants of pulmonic stenosis depending on the location of the obstruction to the

pulmonary valve. ToF is characterized by presenting a subvalvular or infundibular PVS, which causes the thickening of the muscle under the valve, thus narrowing the outflow tract from the right ventricle to the pulmonary artery. However, depending on the degree of PVS, the prognosis of ToF varies, as well as the cyanosis disorder. In that way, if the PVS is mild, the shunt caused by VSD might be left-to-right and the cyanosis may not be present; but if the PVS is severe, which is the case of the classic ToF diagnosis, there is a right-to-left shunt forced by the RVOTO, leading to hypoxia [14].

3) *Right ventricular hypertrophy (RVH)*

The RVOTO causes the hypertrophy of the right ventricle, which alters the size and volume of the heart that becomes typically enlarged "boot-shaped". The hypertrophy appears because the ventricle is required to increase the pressure of distal pulmonary capillaries and veins in order to maintain the pulmonary blood flow and, consequently, decrease the risk of pulmonary edema [13,14].

4) *Overriding aorta*

The aortic valve connects the left ventricle with the aorta. In ToF, the aortic valve is enlarged, which means that the aorta is overridden and thus, it not only arises predominantly from the left ventricle but also from a small part of the right ventricle. This produces a malalignment between the ventricular septum and the aorta, causing this great vessel to override the VSD to different degrees [13].

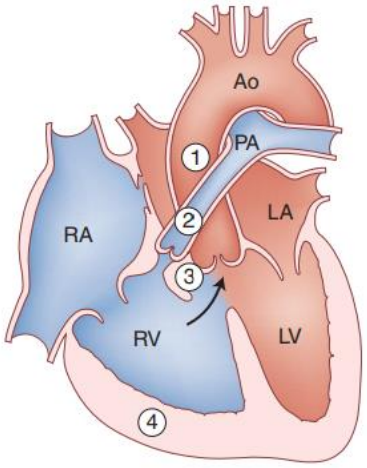

Figure 2. Classical ToF anatomy and its birth defects: (1) overriding aorta, (2) pulmonary infundibular stenosis, (3) ventricular septal defect, (4) right ventricular hypertrophy. (Ao: aorta, LA: left atrium, LV: left ventricle, PA: pulmonary artery, RA: right atrium, RV: right ventricle) [14]

Within all CHDs, ToF causes the highest proportion of in-hospital deaths. Therefore, it is crucial that newborns undergo heart surgery or other procedures soon after birth in order to increase their life expectancy. As a matter of fact, just about 10% of untreated patients survive to 20 years, and just 3% to 40 years, while patients undergoing a complete surgical repair represent a survival rate of 79,6% at 15 years [14].

Regarding the pathophysiology of ToF, it largely depends on the degree of PVS and RVOTO, which is proportional to the grade of cyanosis, as it has already been mentioned [15]. In fact, the severity of ToF relies on the degree of RVOTO, and on the relative pressures in the right and left ventricles, and the proportion of the overriding aorta to the VSD. A representation of the variability of the pathophysiologic effects in ToF depending on the extent of the anatomical defects is shown in *Figure 3*. As can be seen, the more severe the birth defects, the more serious will be the disease, presenting hypoxia, meaning low blood oxygen saturation (SaO_2) [13], which accounts for the measure of how much oxygen the blood carries compared to its maximum. The generally accepted standard states that a normal resting SaO_2 is equal or greater than 95% [16].

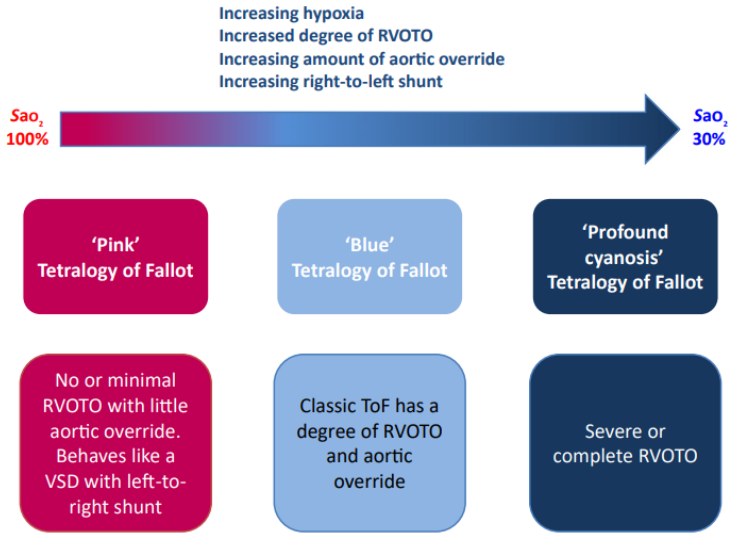

Figure 3. Diagram of the different types of ToF and its pathophysiologic effects [13]

2.1.2) Computational models of the fetal circulation

Modeling of CVS is helpful to understand the complex interactions between different control mechanisms and the hemodynamics of heart and vessels, as well as to comprehend the genesis, development and evolution of cardiovascular diseases and disorders, since it provides computer-based simulations of the different dynamic processes occurring in the system [17].

There are different approaches to simulate the blood flow in the CVS and to help understand its physiological processes. These modeling tools describe the blood behavior with differential equations and are classified according to their domain representations: time domain or frequency domain. Within time domain models there is another classification according to their dimensionality: from 0D to 3D models. While 0D models assume a uniform distribution of blood pressure, flow and volume variables in time within any compartment in the circulatory system (organ, vessel or part of vessel), the higher dimensional ones allow the simulation of the variation of the fundamental variables in space. It is important to state that the specific dimension of the model must be selected taking into consideration the type of study that is being developed and the required level of accuracy [3]. Hence, not necessarily it is better to choose higher-dimensional models for any study that is being realized to provide better diagnostics, physiological understanding, or medical planning [17].

0D lumped parameter models are the simplest ones. They are widely used to understand the circulatory physiology since they offer an accurate way to simulate the blood flow and evaluate the global hemodynamics in the whole circulatory system [3]. Moreover, 0D lumped models have proven to be potentially advantageous for real-time simulation of CHDs on desktop computers, which may be useful for surgical procedure hemodynamic management, although not including specific anatomical information [12]. That way, Broomé et al. [18] presented a real-time lumped parameter cardiovascular simulation model that included the heart and vascular system and allowed simulations of different pathological states. However, identification of patients' initial parameters is an obstacle for bedside simulation that still remains to be solved.

0D lumped models are characterized by representing the fluid dynamics in each compartment of the circulatory system by electric networks [19], these being depicted as a set of simultaneous ordinary differential equations (ODEs) that describe conservation of mass and momentum, and algebraic equilibrium equations that identify the volume of the compartment with the pressure in it [17]. In 0D lumped parameter models, hydraulic-electrical analogy is applied, which establishes an analogy between the blood flow in the circulatory system and the electric conduction in a circuit [3].

Windkessel (WK) model helps to understand the whole arterial system in terms of a pressure-flow relation. It relates the heart and the systemic circulation with a closed hydraulic circuit because it is compared to the maintenance of water pressure in the fire engines [20,21]. *Figure 4* shows this analogy, in which the large elastic arteries act as the WK reservoir [22].

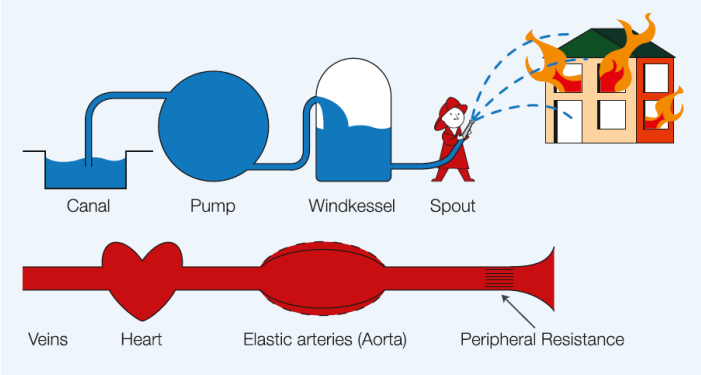

Figure 4. Analogy between the fire engine with the Windkessel and the arterial system [22]

In *Table 1*, there is the correspondence of the hydraulic variables with their corresponding electrical variables. Thus, it is shown that electric circuits can be used to model cardiovascular dynamics. As it is stated, the blood pressure gradient and the voltage gradient act similarly because the first one in the circulatory system pushes the blood to flow against the hydraulic impedance, and the second drives the current to flow against the electric impedance. The hydraulic impedance represents the combination of the effects of blood flow frictional loss resulting from viscous dissipation inside the vessels, inertia of blood, and vessel wall elasticity, which in the case of the electrical impedance, these are represented by a resistance, inductance and capacitance, respectively (RLC networks). In the same way, there is an analogy between blood flow and current laws. The first one is described by three different laws: the continuity equation for the mass conservation, the Poiseuille's law for the steady flow, and the Navier-Stokes equation for the non-steady state. The corresponding analogous laws for the current in a circuit are: Kirchhoff's laws, Ohm's law, and the line transmission equation for the voltage-current relation for high frequencies [17].

Table 1. Variables that characterize the hydraulic network and their electrical analogues

HYDRAULIC	ELECTRICAL
Blood flow (ml/s)	Current (A)
Blood pressure (mmHg)	Voltage (V)
Blood pressure gradient (mmHg)	Voltage gradient (V)
Hydraulic impedance:	Electrical impedance:
- Frictional loss, viscosity (mmHg·s/ml)	- Resistance *R* (Ω)
- Vessel wall compliance (ml/mmHg)	- Capacitance *C* (F)
- Blood inertia (mmHg/ml)	- Inductance *L* (H)

Although 0D lumped models offer a simplified representation of the CVS, their main advantage is that they are easy to solve since they just consist of a set of simple ODEs [23]. However, these models are not able to simulate the non-linearities of cardiovascular mechanics, like the convective acceleration contribution to the system or the non-linear relationship between pressure and volume occurring in a real vessel [3].

The 0D lumped model that simulates the blood flow through the whole CVS, including organs such as the heart, heart valves and veins, consists of different coupled compartments, each one representing one part of the CVS with its mathematical formulas and components, as well as its inflow and outflow points [24]. In that way, 0D lumped models are divided into two subgroups: mono- or single-compartment models, and multi-compartment models. In the first case, the whole arterial network is represented by an electric network [25], and the main objective is to obtain the overall systemic response. On the other hand, multi-compartment models represent separate vascular parts as single-compartment models, which allows the representation of the blood flow spatial distribution in different segments of vessels, and the capture of wave reflections [3,17].

Therefore, the different components that are included in the CVS are modeled as follows:

1) Vascular beds

Vascular beds are modeled with a 3-element WK model, also named Westkessel or RCR model [3], which is displayed in *Figure 5(a)* [26]. It consists of an electric circuit that comprises a capacitor (C_p), which simulates the compliance of the aorta, connected in parallel with a resistor (R_p), which represents the dissipation of small peripheral vessels, and a characteristic impedance (Z_c), which mimics the input impedance for high frequencies [17]. Owing to the behavior of Z_c, a resistor (R_c) is used instead, since they are numerically the same [22].

2) Arterial segments

Segments of the vessel network are modeled with a L-element network, as shown in *Figure 5(b)* [27]. It is a different electrical configuration than that describing the systemic vasculature since their characteristics and properties are dissimilar [17]. It comprises a RLC network and the required boundary conditions are the upstream flow-rate (Q_1) and the downstream pressure (P_2) [27].

3) Valves

Regarding previous 0D lumped models of the heart, there are scientific publications by Pennati et al. [28-31] that present a model of the whole human circulation of the fetus, including the fetal heart, whose aim is the interpretation of local hemodynamic information obtained by non-invasive methods. *Figure 5(c)* shows the electric analog circuit of a ventricle chamber and an arterial valve. As for the valve, it is modeled with an ideal diode connected in series with a non-linear resistor (R_o).

4) Ventricular chambers

Finally, ventricles of the heart are modeled following Pennati et al. publications [28-31]. In *Figure 5(c)* there is the electrical circuit that represents the ventricular chambers, which is comprised by

the isovolumic pressure generator (U), elastance (E) and a ventricular resistance connected in parallel (R_v). It is assumed that left and right ventricles are identical.

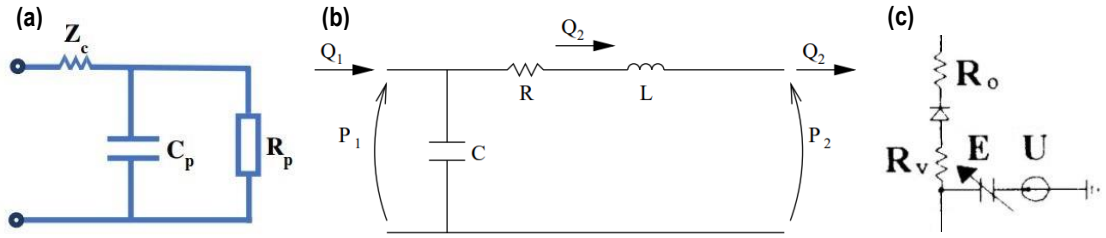

Figure 5. Models that describe the different components of the CVS. a) 3-element WK model – Modification from [26], b) L-element model [27], c) Model of the ventricle and arterial valve – Modification from [28]

Previous 0D lumped models of the fetal CVS have already been studied and published. In [32] and [33], Couto et al. and Huikeshoven et al., respectively, proposed mathematical models of the fetal circulation focused on mimicking the oxygen transport to the fetus. Another fetal circulation model is found in [34], in which the influences of flow pulsations are analyzed, though it presents some shortcomings, such as the simplification of the actual fetal arterial tree and fetal heart's anatomy since it neglects the foramen oval and the ductus arteriosus (DA). Finally, considering a full fetal-placental circulatory model, in [35] Myers et al. proposed a model developed in the frequency domain, a transmission line model in contrast to all the previous presented models that operate in the time-domain, which is why it requires less computational time.

Furthermore, Garcia-Cañadilla et al. has developed different 0D lumped models of the fetal circulation in BCNatal Research Center [36-38], in order to study the blood flow redistribution in fetuses with intrauterine growth restriction (IUGR) and estimate patient-specific vascular properties and hemodynamic parameters which cannot be directly measured in clinical practice. This is going to be explained in the next section.

As previously mentioned, regarding existent 0D lumped models of the fetal heart, there are those published by Pennati et al. [28-31], which focused their study on the fetal CVS modeling, including the four chambers of the heart and the cardiac valves, in order to understand the hemodynamics changes in some fetal diseases. There is a small number of papers proposing models that simulate CHDs [6]. Particularly, there is not any published model of the fetal CVS and hemodynamics of a ToF fetal heart, although there are models that specifically discuss some of the birth defects occurring in ToF in an adult circulatory system. For instance, in [39] there is a model proposed that studies the changes in flow patterns seen in some congenital heart malformations, such as the transposition of the great arteries and VSD. Then, in [40], the Eisenmenger syndrome is simulated, which accounts for a VSD as well. Finally, there is a model that simulates the hemodynamics development in four pulmonary hypertension cases without treatment, one of which is the VSD [41].

2.2) State of the situation

Previous studies have been developed in BCNatal Research Center in order to implement, calibrate and validate a model of the fetal circulation. In 2014, Garcia-Cañadilla et al. [36] developed a 0D lumped computational model of the fetal circulation and its main goal was to

study the blood flow redistribution in fetuses with IUGR. This model was limited only to the fetal arterial tree and, since the fetal heart was not included, the model was directly provided with the boundary conditions of the aortic and pulmonary artery inflow velocities. In this section, this multi-compartment model is going to be discussed since it has been the underlying base of the implemented model within this project. The model of the fetal heart has been designed from scratch, while the simplified vascular circulatory model has been extracted from the mentioned model. Finally, two birth defects occurring in ToF have been also implemented.

Garcia-Cañadilla et al. [36] has shown that computational models are helpful both for understanding blood flow redistribution in IUGR fetuses and for estimating patient-specific properties of the vascular circulatory system, which cannot be directly measured, such as placental resistance and compliance, by means of model personalization using previously measured blood velocity profiles.

The 0D lumped model of the fetal circulation implemented by Garcia-Cañadilla et al. is shown in *Figure 6*, in which there is the anatomical configuration of the circuit *(left)* and its analogue electrical circuit *(right)*. It consists of two main building blocks: arterial segments (highlighted in red solid lines in *Figure 6(b)*) and vascular beds (blue dashed lines).

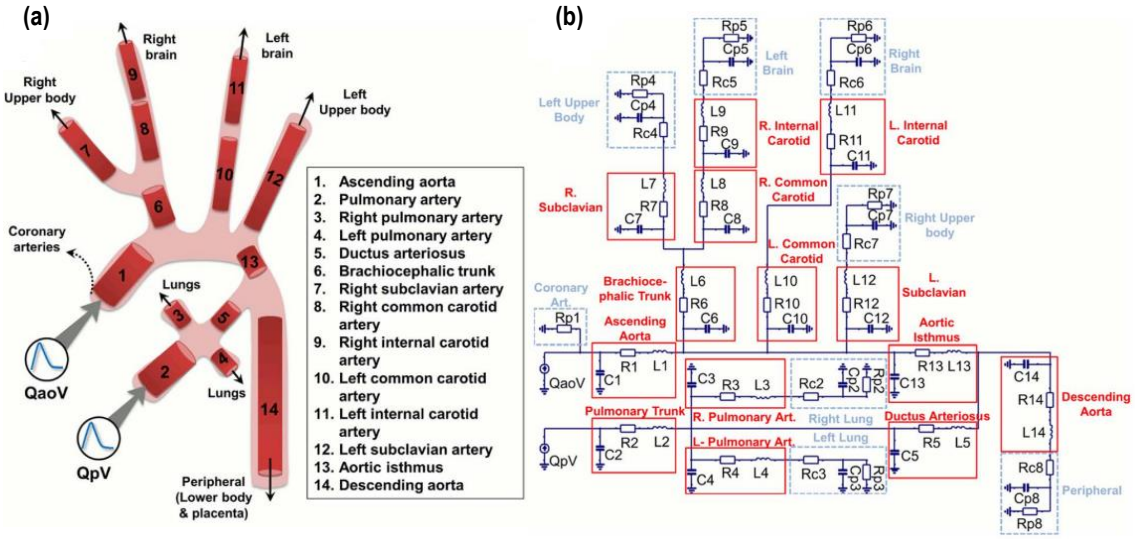

Figure 6. Fetal circulation model: a) Anatomical simplified configuration, and b) Equivalent electrical lumped model [36]

The blocks modeling the arterial segments are composed of three parameters: a resistor *R* that models blood viscosity, a capacitor *C* that models arterial compliance, and an inductor *L* that models blood inertia, corresponding to the L-element network *(Figure 5(b))*. The values of these components are calculated according to the following equations *(Eq. 1, 2, 3)*, which take into consideration the physical dimensions and properties of each vessel:

$$R = \frac{8\mu l}{\pi r^4}; \quad C = \frac{3\pi r^3 l}{2Eh}; \quad L = \frac{pl}{\pi r^2} \qquad (1), (2), (3)$$

where l and r are the length and radius of the arterial segment, μ is the blood viscosity calculated following *Eq. 4*, in which GA corresponds to the gestational age in weeks; E is the

Young's Modulus, h is the wall thickness, assumed to be 15% of r, and p is the blood density (1.05 g·cm^3).

$$\mu = \frac{1.15 + 0.075 \cdot GA}{100} \tag{4}$$

On the other hand, peripheral vascular beds were modelled with a 3-element WK model *(Figure 5(a))*, in which there is a resistor (R_c) connected in series with a capacitor (C_p) and a resistor (R_p) in parallel. The last two components account for the compliance and peripheral resistance of the organs, respectively, whose initial values were extracted from the literature. Besides, the series resistor R_c must equal the characteristic impedance of the local vessel that is feeding the corresponding vascular bed, in order to avoid reflections at high frequencies, as discussed in [12].

Afterwards, in 2015, Garcia-Cañadilla et al. [37] implemented an improved version of the previous model of the fetal circulation by adding new arterial segments and vascular beds and an improved approach to personalize the model to enable the estimation of vascular properties and hemodynamic parameters of each individual, which cannot be directly measured in clinical practice. In this case, regarding the arterial segments, the thoracic and abdominal aorta, and two iliac and two umbilical arteries replaced the descending aorta. Regarding the vascular beds, two kidneys, two lower bodies and placenta vascular bed replaced the peripheral vascular bed.

In this project, a simplified version of the fetal circulation arterial tree has been used, similar to the one proposed in [38]. The anatomical configuration of the designed model consists of 6 arterial segments, including the DA, and 3 vascular beds, which in total sum up to 28 electrical components, together with the left and right ventricles, aortic and pulmonary valves and the two inputs of the system, which consist of the mitral and tricuspid inflows.

3) MARKET ANALYSIS

In this section, a detailed analysis of the current market in which this project belongs to is going to be exposed. It is focused on the different applications that exist nowadays and that have an application in the maternal-fetal medicine, as well as on the possible future perspectives that can be considered taking into account the current situation and technological advances.

3.1) Sectors to which it is addressed

As has been mentioned in the previous sections, the 0D lumped model that is being developed following the memory of this project is destined to the obstetricians, and physicians and biomedical engineers specialized in maternofetal medicine, owing to the fact that its last goal is to provide information about the parameters of the fetus that cannot be measured non-invasively in clinical practice, to improve the detection and prognosis of fetuses with ToF.

In that way, obstetricians with experience invest much time and effort in the delivery planning and the prediction of patient-specific severity of CHDs [41], which is why it is crucial to develop mathematical methods that enable simulations of hemodynamics on a desktop computer [12]. This technological tool could mean a quite important progress in fetal medicine since it is a very innovative method, and it has already provided many advances in this field over the last twenty years [5]. Actually, CHD treatments have demonstrated to require more customized therapies because there is a large inter-patient variability of anatomical and hemodynamic parameters. Hence, *in silico* patient-specific simulation is becoming more important and it has been stated to be a promising tool in the clinical practice to study the hemodynamics of the circulatory system [42].

Computational modeling has been proven to be very powerful and to have a huge potential in many different areas of hemodynamic management. It is useful when aiding CHD understanding, providing clinical decision support, making decisions for surgical procedures, and personalizing treatments, as well as to expand medical imaging data, uncover links between mechanics and biological response [43].

It has already been applied to different CHD diseases, such as patients with univentricular heart, ToF, aortic coarctation, and transposition of the great arteries [5], although those that are being more investigated for mathematical modeling are univentricular heart, and aortic and pulmonary malformations [42].

3.2) Historical evolution of the market

Within current ultrasound technological approaches, fetal echocardiography is the one used in clinical practice to assess alterations in fetal hemodynamics in a non-invasive manner, such as in CHDs. Thus, it is a specialized diagnostic procedure defined as a detailed ultrasound evaluation used to visualize cardiac structures and identify and characterize fetal heart anomalies [44]. Obstetric ultrasound examinations allow real-time ultrasonography. It can be performed with a

transabdominal, transvaginal or transperineal approach, depending on the clinical situation and the needed beam penetration and image resolution. However, transabdominal ultrasonography is generally used to assess the pregnancy since it allows sufficient penetration and provides an adequate resolution [45]. Image quality has improved with advancing technology, as well as obstetricians' techniques and experience, making the identification of the details of the fetal heart anatomy possible [46].

Going back in time, ultrasound examinations were first introduced into medicine in the 1970s. There were rapid technological advances and, from providing static images to enabling real-time images, ultrasound examinations became an indispensable diagnostic method for obstetricians. Thus, in the past three decades, this approach has revolutionized obstetrics [47]. There are various forms of medical diagnostic ultrasound and echocardiography according to its history evolution. M-mode echocardiography was the first developed method which is currently used when temporal resolution is required for precise measurements [48]. Then, two-dimensional (2D) echocardiography, which is stated to be the "gold standard" exam for CHDs diagnosis [48,49], is able to provide real-time images of the heart. Doppler echocardiography was the next cardiac ultrasound method applied in clinical practice, which permits to assess the movement, obtain accurate hemodynamic data and quantify blood flow through vessels. There are different forms of Doppler recordings that are being used in clinical practice, such as color-flow Doppler, which is important for cross-sectional scanning because it enables the visualization of blood flow, and pulsed-wave Doppler, which evaluates diastolic filling patterns and velocities [46,48].

Recent advances in ultrasound examinations involve three-dimensional (3D) and real-time 3D technologies, which were first reported in 1970s but have been limited by the difficulties regarding the acquisition and processing of large imaging data quickly and the data presentation in an understandable 3D format. Nonetheless, although M-mode and 2D echocardiography have enabled to analyze and visualize the heart functioning for more than 30 years, and improvements in 3D echocardiography are still required to optimize its clinical usage, this method represents a promising tool in the contemporary cardiology, particularly in CHDs, since it can depict complex cardiac structures to their realistic forms [46].

During the twentieth century, advances in medicine enabled a paradigm shift of the relationship between physicians and patients. It changed from patient-centric, meaning that it is more concerned on a qualitative sensory inspection of the patient, into a more data-driven approach. Thus, cardiovascular modeling has started to have more impact on clinics [50].

3.3) Future market prospects

Regarding the future perspectives on the use of computational modeling in the clinical environment, it has been proven that it is a rapidly increasing field. Although lumped parameter models cannot substitute clinical exams and judgment, they can be very helpful to guide clinical decisions in surgical and treatment planning, in device placement, and to extend clinical imaging [42], as well as to analyze quantitatively the relationship between hemodynamics and biological processes [43].

However, there are some limitations that must be solved prior to its clinical translation. For instance, although computing power has increased much and modeling now requires hours to complete instead of days, it should enable simulation times in the order of minutes [42]. In addition, it has been stated the need for new technologic tools more focused on physiologic and biologic realism, and clinical utility, thus, clinical trials should put more emphasis on the impact of these tools on patient outcomes rather than on technical demonstrations in case studies. Lastly, design and development of new devices is a favorable promise, which could benefit from computational modeling in order to have both lower cost and lower risk [43]. That way, in a foreseeable future, lumped models are going to be combined with echocardiographic images, so that hemodynamics modeling can be based on specific anatomical data, specifically on CHDs anomalies.

4) CONCEPTION ENGINEERING

This section describes the conception engineering of this project by first describing the data that has been used in order to design and validate the fetal heart 0D lumped model, then explaining the overall pipeline of the project and the methodology that has been followed, and finally presenting some alternative solutions that could have been used instead of a 0D lumped parameter model.

4.1) Study individuals

In order to build and validate the 0D lumped model, clinical and echocardiographic data of healthy fetuses was used. In that way, data from a healthy pregnant women who attended the Maternal-Fetal Department in Hospital Clínic de Barcelona was supplied, which consists of clinical data including GA and estimated fetal weight (EFW); Doppler images from mitral, tricuspid, aortic and pulmonary valves, DA as well as the diameters of the four cardiac valves. From the Doppler images, heart rate (HR), fetal cardiac timing events such as the filling time (FT), isovolumic contraction time (IVCT), isovolumic relaxation time (IVRT), ejection time (ET), and total cycle duration (Tc) were quantified. Moreover, the E (early diastole) and A (late diastole) annular peak velocities of both atrioventricular valves, as well as the aortic and pulmonary maximum blood velocities were also measured. Specifically, data from a healthy fetus of 34.71 weeks of gestation and EFW of 2396 grams was used to calibrate the model and perform all the parametric analyses.

In *Figure 7*, there is an illustration, extracted from [51], of the measured mitral inflow and aortic outflow of the left heart of a fetus during a heart beat together with all the timings: FT, IVCT, ET and IVRT. In it, there can be clearly observed the specific waveform of the biphasic inflow that is generated by the entering of blood to the ventricle by means of the atrioventricular valve opening. This includes the E (early or passive diastole) wave that represents the myocardial relaxation in which the blood from atria fills the ventricle due to pressure differences, and the A (atrial, active or late diastole) wave that depicts the atrial contraction during ventricular filling. Moreover, the division of the cardiac cycle into its four different time periods is also displayed:

- FT: It consists in the diastolic or ventricular filling stage, in which blood flows from atria to ventricular chambers, and it occurs after the mitral and tricuspid valves opening. It comprises E diastole and A contraction period.
- IVCT: The next period occurs after the atrioventricular valves closure and just before the aortic and pulmonary valves open, in which the systole begins, thus the ventricular pressure starts increasing.
- ET: The opening of arterial valves is forced by the increase in ventricular pressure, which causes the ejection of blood to the arterial vessels.
- IVRT: It comprises the beginning of the diastole period, in which the myocardium starts relaxing. It happens within the closing of the aortic and pulmonary valves and the opening of the atrioventricular valves.

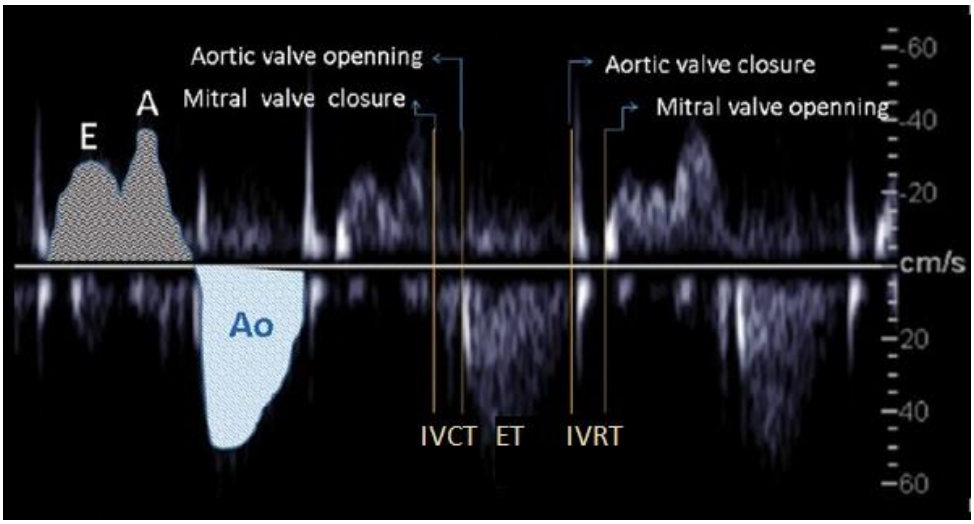

Figure 7. Mitral biphasic inflow (E and A waveforms) and aortic outflow (Ao waveform) in a spectral Doppler image. Time intervals include: IVCT, ET, and IVRT – Modification from [51]

4.2) Proposed Solution

In this project, a mathematical model of the fetal heart and part of the vascular circulatory system has been developed using MATLAB environment and Simulink which enables the modeling and simulation of dynamic systems in a graphical interactive editor. Indeed, Simscape Electrical™ toolbox has been used in order to implement the electric circuit.

As it will be discussed in the following sections, the final simplified 0D lumped model involves two different parts: the heart and the vascular system. The first one consists of the left and right ventricles and the aortic and pulmonary valves of the heart, and it includes two input functions corresponding to the mitral and tricuspid inflows. The second part comprises 6 arterial segments, which include the ascending aorta, thoracic aorta, DA, main pulmonary artery and left and right pulmonary arteries, and 3 vascular beds: the systemic circulation and left and right pulmonary circulation. In addition, since it is not a closed model, thus the venous circulation was not modeled, the venous pressure was considered 0 mmHg. Therefore, all the peripheral resistors and capacitors were connected to ground.

The first step was the design of the fetal heart 0D lumped model, including only the two ventricles and the two arterial valves (aortic and pulmonary valves). The two atria were remodeled since the mitral and tricuspid valve inflows were used as input of the proposed model. These fluxes and the composition of the heart model are mostly based on papers published by Pennati et al., specifically in [30], where the required equations are provided. Then, a simplified version of the vascular circulatory system was integrated into the model, based on the modeling approach published by Garcia-Cañadilla et al. [36-38]. That way, the systemic and the pulmonary circulations join through the DA arterial segment.

In addition, owing to changes in the vascular compliances and resistances, as well as in some hemodynamic parameters, that occur during fetal growth, their values must be scaled considering the EFW of the fetus. By means of different allometric equations proposed by Pennati et al. in

[52], vascular and cardiac parameters of the human fetus can be directly associated to the fetal weight, which is related to the anatomical dimensions of vessels.

Then, once the model was adjusted in healthy conditions, parametric sensitivity analysis was performed in order to quantify the relative importance of the different input cardiac parameters on the model output. The next step was the calibration of the 0D lumped model, which included the fetal heart and the vascular circulation, to guarantee that the computational outcomes fit with the patient-specific measurements. Thus, a set of different parameters was calibrated, using an automatic optimization-based calibration method implemented in MATLAB. The algorithm returned an association of parameter values that gave the minimum possible error between the simulations and the real data. Finally, having the fetal heart model calibrated, two of the birth defects present in ToF, which are VSD and PVS, were modeled and the effects they cause to the hemodynamics were analyzed by means of parametric analysis.

4.3) Alternative solutions

As has been previously discussed in section 2.1.2, the models in time domain are classified depending on their dimensionality. This project has focused on 0D lumped models, but it is important mentioning the properties of the higher dimensional ones and why a lower dimension model has been adopted.

A summary of the properties of the models in the different dimensions in time domain is shown in *Table 2*, extracted from [3]. While 0D lumped models consider a uniform distribution of the fundamental variables in space at any time, higher dimensional ones (1D, 2D and 3D models) do allow the recognition of the variation of these parameters in space. Therefore, 0D models just enable the simulation of pressure and flow changes in local areas of circulation. On the other hand, 1D models permit the representation of the effect of the wave reflection, and they describe the variation of the flow velocity through the length of the blood vessel. 2D models can describe the radial changes of blood flow occurring in a tube with axial symmetry. Finally, 3D models are required when the flow must be represented in 3D domains, such as in bifurcations of vessels, through heart valves, or inside ventricles [3,10].

Blood flow behaves differently according to its location in the CVS, so it is important to have a model that enables the representation of the spatial distribution. Although 0D lumped models are uniform in space, spatial distribution can be approximated by implementing multi-compartment models, in which blood flow and pressure remain constant in each compartment [10]. Therefore, more complex (higher-dimensional) models do not have to be used in this project because they would add unrequired complexity and are computationally very expensive compared to 0D lumped models. In addition, it is well known that 0D lumped models are appropriate for the study and evaluation of the hemodynamic interactions among different cardiovascular organs, as of the global distribution of variables for specific physiological conditions [3], which applies for the main objective of this project. These are the main reasons why we decided to implement a 0D lumped parameter model, whose validity in describing the CVS is supported by a great number of publications already available in the literature [29].

Table 2. Comparison of modeling techniques in time domain for the study of cardiovascular dynamics

METHOD OF STUDY		SUITABLE RESEARCH TARGET
Lumped parameter model	0D	- Global cardiovascular dynamics in the whole CVS - General pressure and flow-rate changes in a local circulation loop - Possibly to provide boundary conditions for local 3D models
Distributed parameter model	1D	- Pulse wave transmission - Improved boundary conditions for 3D local models, capable of capturing systemic wave reflection effects
	2D	- Local flow field study in axisymmetric domains - Further improvement of boundary conditions for local 3D models, but limited applicability
	3D	- Local flow field study in full 3D domains

5) DETAILED ENGINEERING

In this section of the project report, a detailed explanation of the development of the study and the different steps and methodology is presented. First, a brief definition of the input data used to build the model is described. Then, the anatomical configuration and the equivalent electric circuit of the final designed model, together with the description of each of its components are described, including the model of the VSD. Finally, the description of the parametric analysis, the patient-specific calibration of the model in healthy conditions, and the parametric studies to evaluate the hemodynamic changes due to different size / degree of VSD / PVS are provided.

5.1) Input Data

The clinical and echocardiographic data of a healthy fetus used to implement and calibrate the model is shown in *Table 3*.

Table 3. Specific clinical data of a patient from Hospital Clínic de Barcelona (EFW: estimated fetal weight, GA: gestational age, FT: filling time, IVCT: isovolumic contraction time, ET: ejection time, IVRT: isovolumic relaxation time, T_c: total cycle duration, HR: heart beat, E: early or passive diastole, A: atrial, active or late diastole)

CLINICAL PARAMETERS		MEASURED DATA	
Clinical	EFW (g)	2396	
	GA (weeks)	34.71	
Timings	FT (ms)	0.20	
	IVCT (ms)	0.035	
	ET (ms)	0.204	
	IVRT (ms)	0.02	
	T_c (s)	0.458	
	HR (bpm)	136.5	
		LEFT HEART	***RIGHT HEART***
Velocities	E (cm/s)	34.7	45.1
	A (cm/s)	46.2	57.0
	Arterial Valve Peak Vel. (cm/s)	92.0	81.0
Diameters	Atrioventricular Valve diameter (mm)	13.1	13.7
	Arterial Valve diameter (mm)	5.4	6.7

The blood flow inputs, which are the mitral and tricuspid valves' flows, are calculated from the velocities using the following equation: $Q = V \cdot \pi \cdot r^2$, where r is the valve radius, and V is the blood velocity function. A MATLAB script has been developed to compute the mitral and tricuspid blood velocities, using the E and A annular peak velocities from both valves, the FT, and the whole cardiac cycle duration *(see Table 2)*. The diameters of the atrioventricular valves have been slightly modified to achieve a more accurate model performance. In *Figure 8*, both computed velocity profiles are represented, whose biphasic waveforms can be compared to the ones previously seen in *Figure 7*.

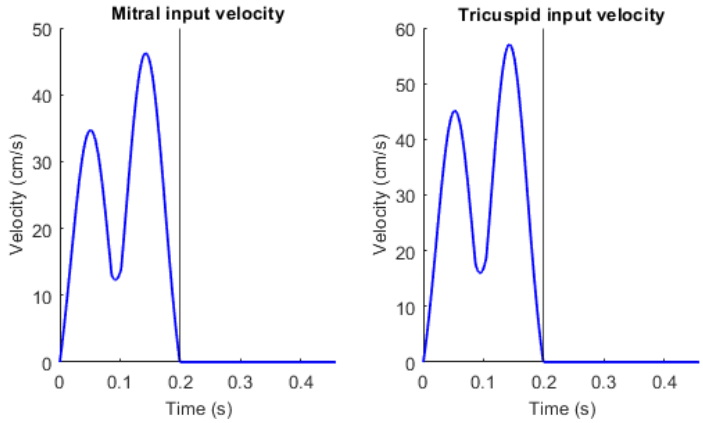

Figure 8. Computed atrial input velocity, from left and right atria, respectively

5.2) Fetal heart 0D lumped parameter model with and without cardiac defects

The 0D lumped model of the heart and CVS of a fetus that was finally implemented is shown in *Figure 9*, which accounts for its anatomical configuration and the electric analogue circuit.

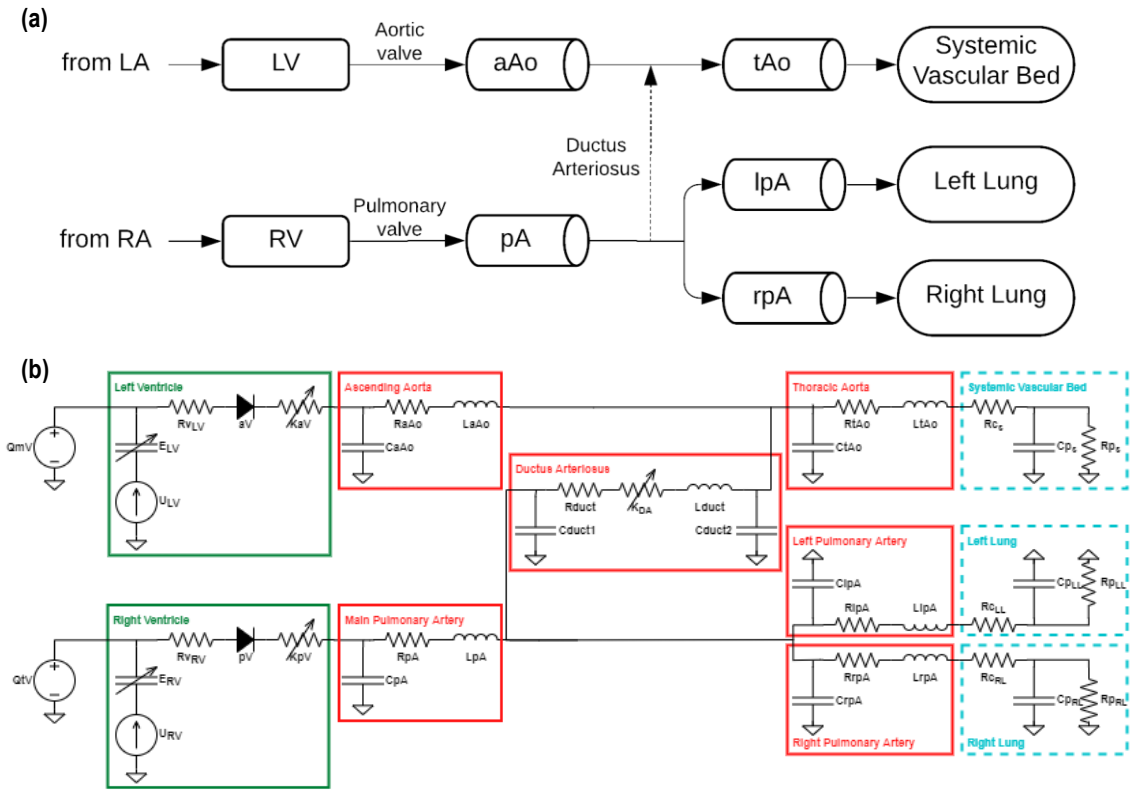

Figure 9. 0D lumped model of a normal fetal heart. a) Anatomical configuration of the model, b) Equivalent electric circuit (LA: left atrium, LV: left ventricle, RA: right atrium, RV: right ventricle, aV: aortic valve, pV: pulmonary valve, aAo: ascending aorta, tAo: thoracic aorta, pA: main pulmonary artery, lpA: left pulmonary artery, rpA: right pulmonary artery, QmV: mitral valve flow, QtV: tricuspid valve flow, U: isovolumic pressure generator, E: elastance, s: systemic vasculature, LL: left lung, RL: right lung, DA/duct: ductus arteriosus)

Figure 9(a) shows a scheme of the anatomy of the model, in which we can see all the components previously mentioned: both inputs, left and right ventricles, the arterial valves, the 6 arterial segments, including the fetal shunt (dashed line), and the 3 vascular beds.

On the other hand, *Figure 9(b)* shows the equivalent electric circuit of the model. It includes both ventricles and arterial valves (highlighted in solid green lines), modelled with an isovolumic pressure generator, an elastance term and a resistance connected in parallel, and an ideal diode with a non-linear resistance in series, respectively *(Figure 5(c))*; the arterial segments (highlighted in solid red lines), all of them modeled following the L-element model *(Figure 5(b))*, and the DA presenting a slight modification to the previous network because it presents two compliances instead of just one; and finally, the vascular beds (highlighted in dashed blue lines), modelled with a 3-element WK *(Figure 5(a))*. Next, the different components of the model are going to be described.

5.2.1) Ventricles of the heart

With respect to the modeling of the fetal ventricles, these are modelled after Avanzolini et al. [53], and discussed thoroughly by Pennati et al. [28-31]. Three components are required: isovolumic pressure generator $U(t) = U_0 \cdot A(t)$, which takes into account the contractile properties of the myocardium, a resistance Rv, which is a constant viscous term related to the dissipative viscosity of the myocardium wall, and the elastance, described by Zhu et al. in [54] as $E(t) = E_{dia} + (E_{sys} - E_{dia}) \cdot e_n$, a time-varying elastic term which is associated to the elastic characteristics and the geometry of the ventricle and that relates the ventricular pressure with the ventricular volume. In these relationships, U_0 is the isovolumic pressure generator constant; E_{dia} and E_{sys} are the diastolic and systolic ventricular elastances, respectively; e_n represents the normalized elastance; and $A(t)$ is the normalized sinusoidal activation function that describes the progressive fiber excitation-relaxation pattern of the ventricles as follows:

$$A(t) = \begin{cases} \dfrac{1 - cos\left(\dfrac{2\pi t}{T_s}\right)}{2} & 0 \le t \le T_c \\ 0 & T_s < t < T_c \end{cases} \quad (5)$$

where T_c and T_s are the cardiac and systolic time duration, respectively.

The final values of the different parameters adopted for the implemented heart model are provided in *Table 4*. It must be mentioned that, as the fetal heart grows during the gestation, it suffers from anatomical, mechanical and functional changes due to substantial structural modifications on the myocardial tissue. Pennati et al. [47] defined a scaling approach of human fetal cardiac and circulatory parameters in order to consider the increase of the fetal body size during human gestation. The adopted expression is the allometric equation shown in *Eq. 6* and it describes the changes in the parameters as a function of the EFW:

$$Y_i = Y_0 \cdot (W_i/W_0)^b \quad (6)$$

where b is the scaling factor and describes the effect of a change in body size, Y_i is the variable under study which is scaled for the EFW, Y_0 is the reference arterial dimension of a specific EFW and GA, W_i is the EFW of the patient being studied in grams, and W_0 is the reference EFW which is calculated as $log_{10}(W_0) = 0.2508 + 0.1458 \cdot GA - 0.0016 \cdot GA^2$ [55].

It has been demonstrated that the contractile parameter U_0 is lower in a fetus heart near term than in an adult heart, while the elastances E_{dia} and E_{sys} are higher. This means that the

isovolumic pressure generator constant increases during pregnancy and elastances decrease [55]. We extracted values of these three parameters from Pennati et al. [29], which are U_0 = 40 mmHg, E_{dia} = 0.3 mmHg/ml and E_{sys} = 3.0 mmHg/ml, corresponding to a fetus of 3 Kg. The scaling factors (b) of the allometric equation *(Eq. 6)* for U_0, E_{dia} and E_{sys} were 0.1, – 0.8 and – 1.1 respectively, and were obtained from [55]. Regarding the ventricular resistance R_v, it undergoes the same behavior as the rest of the vessels' resistive terms which are assumed to decrease when the body weight increases. Therefore, the initial value of R_v = 0.08 mmHg·s/ml, and the corresponding scaling factor is -1.0 [55]. Hence, the final adopted values are given in *Table 4*.

Figure 10(a) shows the course of $A(t)$ during a cardiac cycle. The initial values considered for T_s and the delay between the atrial and the ventricular systoles are 0.22 and 0.10 seconds, respectively. These two parameter values are going to be adjusted for the patient-specific calibration. On the other hand, in *Figure 10(b)*, the elastance curve $E(t)$ is represented.

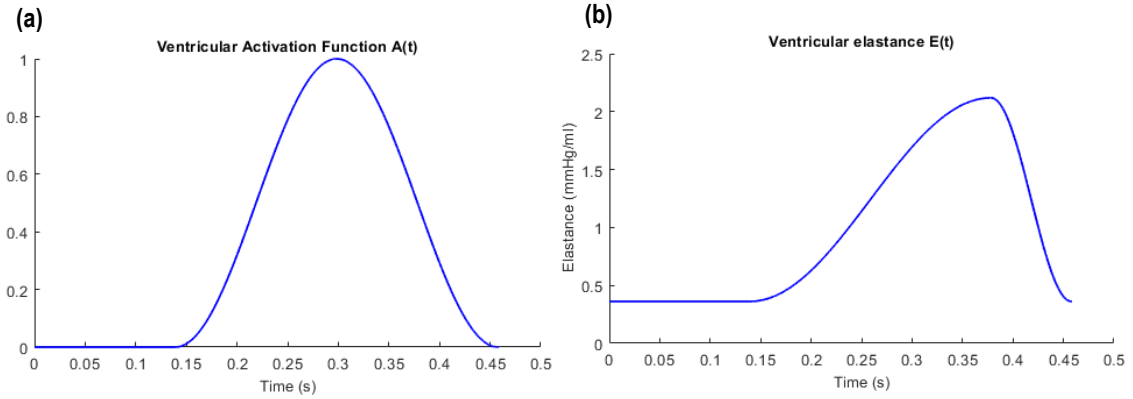

Figure 10. a) Activation function of the fetal ventricles; b) Time-varying elastance of the fetal ventricles

5.2.2) Aortic and pulmonary valves

Cardiac valves are modeled with two components connected in series: an ideal diode that limits flow to one direction, and a non-linear resistor that describes the non-linear relationship accounting for the dissipative properties of the heart, as previously described *(Figure 5(c))*. Two custom blocks have been designed in Simscape, MATLAB, to implement these two components.

Regarding the design of the diode, it was based on the mathematical model in [56], which accounts for a model that includes the heart and valves but using hydraulic instead of electric components. The diode's behavior that enables one-way blood flow is characterized as follows:

$$i = \begin{cases} \dfrac{V_+ - V_-}{R_{diode}} & if\ V_+ \geq V_- \\ 0 & otherwise \end{cases} \quad (7)$$

where i is the current that simulates the valves' flow, $V_+ - V_-$ is the voltage difference representing the pressure drop across them, and R_{diode} is a small resistor, whose value is listed in *Table 4*.

The non-linear relationship of cardiac valves is described by Yellin et al. [57], and again discussed by Pennati et al. [28,31] and by Shimizu [12], and it follows the next expression:

$$V_+ - V_- = R_{valve} \cdot i^2 \quad (8)$$

where R_{valve} is a dissipative component that depends on the valvular diameter, thus it is computed following *Eq. 1* that depends on the physical dimensions of each valve. Their length is 1 mm and their diameters are shown in *Table 3*.

Table 4. Parameter values used in the fetal heart model of this project

PARAMETER	VALUE
U_0 (mmHg)	39.078
E_{sys} (mmHg/ml)	3.877
E_{dia} (mmHg/ml)	0.362
R_v (mmHg·s/ml)	0.101
R_{diode} (mmHg·s/ml)	0.001

5.2.3) Systemic and pulmonary circulations

The resistance, compliance and inductor components of the arterial segments, which are the ascending aorta, thoracic aorta, main pulmonary artery, left and right pulmonary arteries and DA, are set up following *Eq. 1,2,3* described in section 2.2, respectively. Besides, the values of the two capacitors of the DA have been adjusted by dividing the value of a single capacitor by two.

The physical dimensions of each vessel are required to compute the values of the previous electric components. These are calculated according to the specific GA of the fetus, as shown in *Table 5*.

Table 5. Equations describing the vessel's physical dimensions (length, diameter and E: Young's modulus) as a function of gestational age in weeks for the 6 arterial segments included in the final lumped model

VESSEL	LENGTH (mm)	DIAMETER (mm)	E ($g \cdot cm^{-1} \cdot s^{-2}$)
Ascending aorta + Aortic arch	$-4.678 + 0.465 \cdot GA + -6.079 + 0.637 \cdot \mathrm{GA}$	$-2.103 + 0.2684 \cdot GA$	$1.69 \cdot (3.8 \cdot 10^2 \cdot GA^2 + 4.7 \cdot 10^3 \cdot GA + 1.5 \cdot 10^4)$
Main pulmonary artery	$-5.604 + 0.571 \cdot GA$	$-2.77 + 0.30 \cdot GA$	$1.69 \cdot (3.8 \cdot 10^2 \cdot GA^2 + 4.7 \cdot 10^3 \cdot GA + 1.5 \cdot 10^4)$
Right pulmonary artery	$-4.00 + 0.41 \cdot GA$	$-1.71 + 0.18 \cdot GA$	$1.69 \cdot (3.8 \cdot 10^2 \cdot GA^2 + 4.7 \cdot 10^3 \cdot GA + 1.5 \cdot 10^4)$
Left pulmonary artery	$-4.00 + 0.41 \cdot GA$	$-1.95 + 0.19 \cdot GA$	$1.69 \cdot (3.8 \cdot 10^2 \cdot GA^2 + 4.7 \cdot 10^3 \cdot GA + 1.5 \cdot 10^4)$
Ductus arteriosus	$-3.073 + 0.438 \cdot GA$	$\frac{-0.166 + 0.121 \cdot GA}{0.798 + 0.003 \cdot GA}$	$3.04 \cdot (3.8 \cdot 10^2 \cdot GA^2 + 4.7 \cdot 10^3 \cdot GA + 1.5 \cdot 10^4)$
Thoracic aorta	$-19.654 + 2.051 \cdot GA$	$-2.383 + 0.237 \cdot GA$	$2.02 \cdot (3.8 \cdot 10^2 \cdot GA^2 + 4.7 \cdot 10^3 \cdot GA + 1.5 \cdot 10^4)$

Once the physical properties were calculated according to the GA of the fetus, they were scaled using the allometric equation *Eq. 6*. For any anatomical linear quantity, like the human fetal

vessel lengths and diameters, a scaling factor (b) of 0.33 can be used to describe the changes occurring during pregnancy [47].

With regard to the vascular beds, these consist in a resistor (R_C), and a peripheral capacitor (C_p) and resistor (R_p). As for the R_C, it must equal the characteristic impedance of the vessel that is feeding the vascular bed in order to avoid wave reflections. Concerning the R_p and C_p of the systemic and pulmonary circulations, the initial values listed in *Table 6*, which were extracted from the previous models of BCNatal research group, were adopted. Right and left lungs were assumed to be identical, so they were given the same parameter values. In the next sections, we are going to discuss the calibration of these values.

Table 6. Initial values of peripheral resistances and compliances

PARAMETER	VALUE
R_{lungs} (mmHg·s/ml)	36.2369
R_s (mmHg·s/ml)	4.0677
C_{lungs} (ml/mmHg)	0.0516
C_s (ml/mmHg)	0.0935

5.2.4) Fetal heart model with VSD and PVS

The VSD was modeled with a linear resistor that connects both ventricles. The model of the fetal CVS including the VSD is displayed in *Figure 11*. As discussed in [12], it is not necessary to use non-linear components in order to simulate a VSD. Therefore, the value of this resistance is calculated following the *Eq. 1*, using the size of the defect as the diameter. As for the length of VSD, it corresponds to the septal wall thickness. García-Otero et al. [58] constructed nomograms for different fetal cardiac dimensions and myocardial wall thicknesses. The corresponding regression equation against GA for the septal wall thickness is $-0.468 + 0.117 \cdot GA$, which results in a value of 4.151 mm for the VSD length. Finally, we have kept the value for the blood viscosity constant.

Regarding the PVS, this has been simulated by reducing the diameter of the pulmonary valve from the 0D lumped model in healthy conditions.

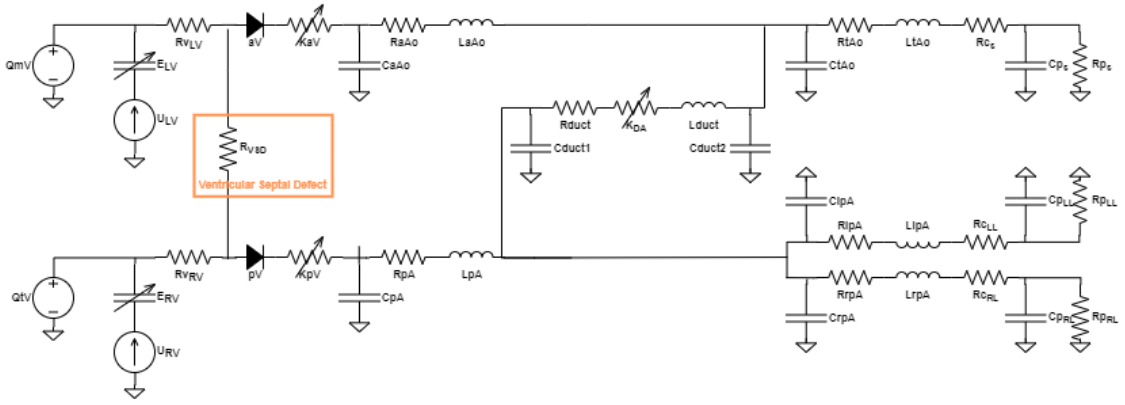

Figure 11. Equivalent electric circuit of a fetal heart with VSD. (QmV: mitral valve flow, QtV: tricuspid valve flow, U: isovolumic pressure generator, E: elastance, LV: left ventricle, RV: right ventricle, aV: aortic valve, pV: pulmonary valve, aAo: ascending aorta, tAo: thoracic aorta, s: systemic vasculature, pA: main pulmonary artery, lpA: left pulmonary artery, rpA: right pulmonary artery, LL: left lung, RL: right lung, DA/duct: ductus arteriosus)

5.3) Parametric analysis in healthy conditions

Parametric sensitivity analysis allows us to examine how a model behaves as you vary one or more of its input parameters. In this project, multiple single parametric analyses were done to inspect the individual contribution of each selected model parameter to the whole system and evaluate its performance to mimic blood flow velocities and pressures in the fetal heart.

The selected input parameters for the parametric analysis were: the four organ peripheral resistances and compliances (R_p, C_p) of the systemic circulation and pulmonary circulation vascular beds, the ventricular contraction duration (T_v), the delay between the atrial and the ventricular contraction ($delay$), and the diameters of both mitral and tricuspid valves ($d_{mitral}, d_{tricuspid}$). The initial values for the R_p and C_p of both pulmonary and systemic circulations, and the T_v and $delay$ have been just discussed in section 5.2. Regarding the mitral and tricuspid valve diameters, we have chosen different initial values instead of using those provided in *Table 3*. There is high variability in the clinical measurement of cardiac valve diameters, and its accuracy is influenced by different factors, such as image resolution, the echocardiographer performing the measurement, and even the specific type of echocardiographic equipment and imaging transducer used [59]. In this case, we finally determined that the values given for the atrioventricular valve diameters of the healthy patient *(Table 3)* were significantly different from those extracted from literature, which was likely to introduce some error in the model. Thus, we used the values given in [29], which were extracted from [60] by De Smedt et al., that is 9 and 9.3 mm for the mitral and tricuspid valves, respectively, corresponding to a fetus with a EFW of 3 Kg. Then, the allometric equation *Eq. 6* with a scaling factor equal to 0.33 was used in order to scale both diameters to the EFW of the healthy patient (*Table 3*), resulting in 8.33 and 8.61 mm for the mitral and tricuspid valves, respectively. The rest of the model parameters were set to their corresponding nominal value, provided in the previous sections.

For each of the 8 selected parameters, a range of 10 possible values were defined, covering values either below and above its nominal value, providing that it is an appropriate range to include all the possible physiological values in healthy conditions. The minimum and maximum values for each parameter are shown in *Table 7*. In the case of T_v and delay parameters, the range has been defined taking into account that the expression $T_v + delay \leq T_c$ is fulfilled.

Table 7. Minimum and maximum values for peripheral resistances and compliances, ventricular systolic time and time delay between atrial and ventricular systole, and diameters of atrioventricular valves

PARAMETER	VALUE	
	Min.	Max.
R_{lungs} (mmHg·s/ml)	2.416	72.474
C_{lungs} (ml/mmHg)	0.001	0.206
R_s (mmHg·s/ml)	0.407	12.203
C_s (ml/mmHg)	0.0006	0.125

PARAMETER	VALUE	
	Min.	Max.
T_v (seconds)	0.11	0.352
$delay$ (seconds)	0.05	0.23
d_{mitral} (mm)	5.0	16.67
$d_{tricuspid}$ (mm)	5.18	17.28

5.4) Calibration of the simplified model of the fetal heart in healthy conditions

Following the sensitivity analysis that has enabled to understand and evaluate the individual contribution of a set of 8 parameters on the resulting pressure and flow waveforms, the next step is the calibration of the model using the clinical and Doppler data from the healthy control fetus described in section 5.1. The main goal of this section is to adjust the model parameters to fit the model-based velocity waveforms of the aorta (V_{aorta}), main pulmonary artery (V_{pulm}), and DA (V_{DA}), and the values of the different cardiac timings: FT, IVCT, ET and IVRT, to the measured ones *(Table 3)*, as well as to ensure that the values of the systolic blood pressure (SBP), diastolic blood pressure (DBP) and mean blood pressure (MBP) are within the corresponding physiological values that are described by Struijk, P. C. et al. in [61], computed as follows:

$$SBP\ (mmHg) = 1.06 \cdot GA + 15.91 \tag{9}$$

$$DBP\ (mmHg) = 0.67 \cdot GA + 2.47 \tag{10}$$

$$MBP\ (mmHg) = 0.87 \cdot GA + 10.33 \tag{11}$$

In the case of the SBP, DBP and MBP values corresponding to the presented healthy patient *(Table 3)*, these are 52.70, 25.73 and 40.53 mmHg, respectively. With respect to MBP, this is computed following the equation: $MBP = (1/3) \cdot SBP + (2/3) \cdot DBP$ [61].

The subset of 8 model parameters that were selected for the model calibration because they needed to be adjusted were: the pulmonary and systemic circulation vascular beds, the heart parameters T_v and delay, and the mitral and tricuspid valve diameters, as explained in section 5.3.

For a better performance of the optimization algorithm, the variation of the model parameters with respect to their nominal values was estimated. Optimization process was done using a constrained nonlinear optimization algorithm (*surrogateopt* function from MATLAB [62]) that minimizes an objective function denoted by *J*. The optimization algorithm iteratively varies the model parameters until the objective function reaches a minimum value. The initial values of the model parameters that had to be provided to the optimization algorithm were randomly chosen within a physiological range. The objective function was defined as the weighted sum of the relative errors between the model-based (denoted by ~) and the real variables, as shown in the following expression:

$$J = \frac{1}{9} \cdot \left(\sum_{i=aorta,pulm,DA} NRMSE\left(V_i, \tilde{V_i}\right) + \sum_{k=SBP,DBP,MBP,FT,IVCT,ET} RMSE\left(k, \tilde{k}\right) \right) \tag{12}$$

where i indicates the three different locations of the fetal circulation where blood velocity was measured (aorta, pulmonary artery and DA), and k corresponds to the other six cardiac parameters (systolic, diastolic and mean blood pressures and cardiac timings) that had also been calculated or measured. The relative error of the blood velocities profiles was computed using the normalized root-mean-square error (NRMSE), while the relative error of the rest of single variables were computed using the root-mean-square error (RMSE).

5.5) Parametric analysis of the fetal heart model with VSD and PVS

Once the model was calibrated under healthy conditions, we modeled two of the cardiac defects present in ToF: VSD and PVS. In section 5.2.4, the 0D lumped parameter model that includes both defects was described. In this section, two parametric analyses were performed in order to evaluate the effects of both defects on the fetal hemodynamics.

Regarding the VSD, as it has been previously explained in section 5.2.4, this is modeled by a linear resistor that connects both left and right ventricles, and the value of this electric component was adjusted taking into account its physical dimensions *(Eq. 1)*. The VSDs are often classified as small, if the diameter is ≤ 3 mm; medium, if the diameter ranges from 3 to 6 mm; and large, if the diameter is > 6 mm [63, 64]. Therefore, a range of 10 values from 1 to 10 mm corresponding to the VSD diameter was defined.

With respect to the PVS, this was modeled by decreasing the value of the pulmonary valve diameter, which is required to compute the dissipative coefficient of the valve's non-linear resistor that is consequently modified. Therefore, to study the effects of different degrees of PVS on fetal hemodynamics, a range of 8 decreasing factors from 0.9 to 0.2 with respect to its original size was defined. PVS severity is quantitatively assessed by the transpulmonary pressure gradient and the velocity flow curve across the pulmonary valve. The pressure gradient is derived from the velocity profile, using the simplified Bernoulli equation $\Delta P = 4v_{max}^2$, which has proven to be reliable thus it has good correlation with invasive measurement using cardiac catheterization [65]. American College of Cardiology/American Heart Association (ACC/AHA) published in 2006 the classification of PVS, in adults, in terms of the peak velocity and the peak gradient, as shown in *Table 8* [66]. In the case of fetuses, we have not found literature giving specific values for the grading of PVS severity, although in [67] they use this classification for neonates with PVS. Then, in [68], Castor et al. demonstrated that the Doppler-derived pressure gradient and the peak Doppler velocities can be misleading in the assessment of PVS severity during fetal life, if used alone, and that they are useful for the identification of mild to moderate forms of stenosis but must be used with extreme discretion for more severe cases, since it was proven that they did not increase systematically in proportion to the severity of the stenosis. However, this table can provide a first insight into the hemodynamic changes in a fetal heart with PVS.

Table 8. Grading of PVS severity

	Mild	Moderate	Severe
Peak velocity (m/s)	<3	3 – 4	>4
Peak gradient (mmHg)	<36	36 – 64	>64

6) RESULTS AND DISCUSSION

The results of the study are presented in this section, along with their corresponding discussion. Following the steps of the project that have already been explained, first the resulting plots of the different parametric analyses are exposed; then the results of the calibration of the 0D lumped model of the fetal heart are shown and, finally, an estimation of the effects of different VSD sizes and degree of PVS on fetal hemodynamics is depicted.

6.1) Parametric analysis in healthy conditions

6.1.1) Peripheral resistances and compliances of pulmonary and systemic vascular beds

In *Figure 12*, it is shown the single parametric study of the variation of the peripheral compliance of the pulmonary circulation vascular bed (C_{lungs}) in the healthy fetus (*k* is the changing factor that multiplies the parameter's nominal value). The model-based pressure waveforms in left *(Fig.12(a))* and right *(Fig.12(b))* ventricles are plotted, as well as the velocity profiles in the aorta, pulmonary artery and DA *(Fig.12(c,d,e))*. The resulting plots of the variation of the systemic circulation vascular bed peripheral compliance (C_s), and both the pulmonary and systemic circulation vascular bed peripheral resistances (R_{lungs}, R_s) are presented in Appendix A.

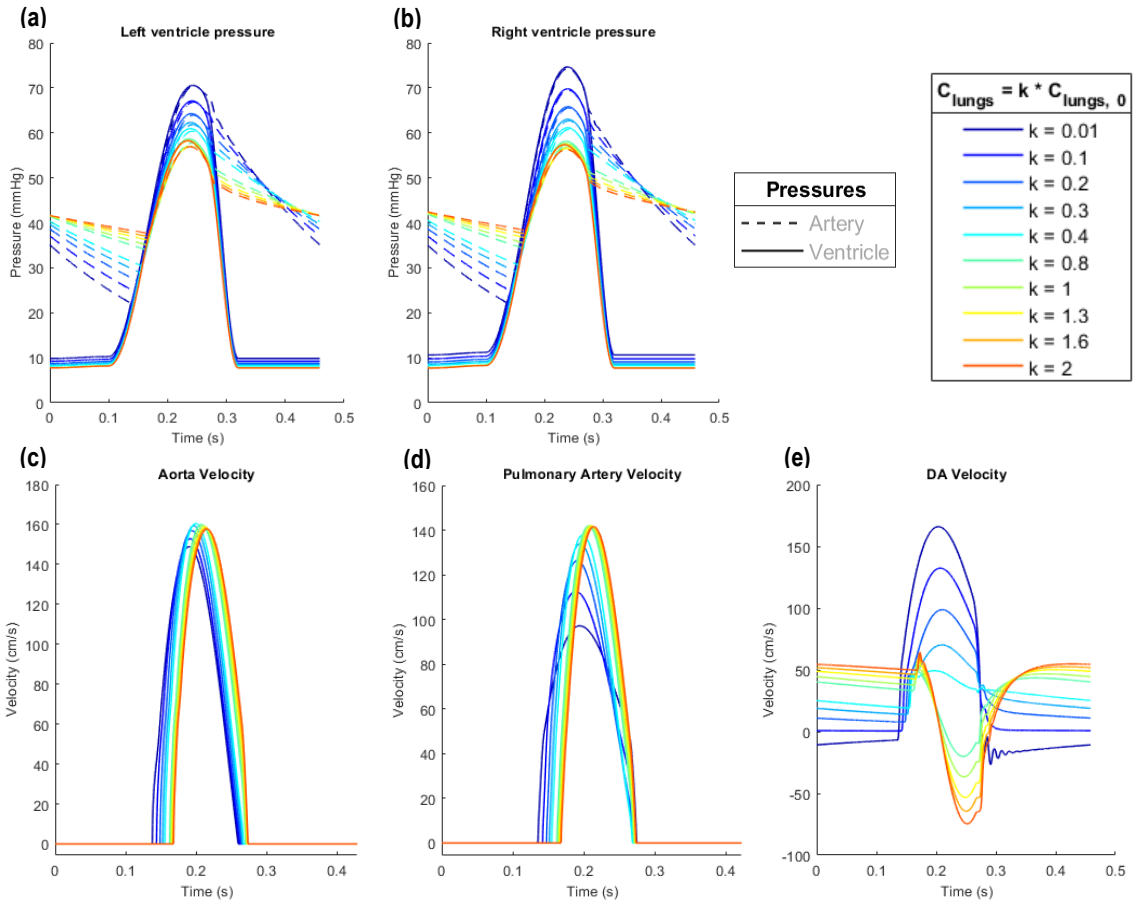

Figure 12. Model-based waveforms resulting from the parametric study on the variation of the peripheral compliance of the pulmonary circulation vascular bed (C_{lungs}): a) left ventricle and aorta pressure; b) right ventricle and pulmonary artery pressure; c) aorta velocity; d) pulmonary artery velocity; e) DA velocity

The obtained results suggested that by increasing the value of C_p (both pulmonary and systemic circulation vascular bed compliances) *(Fig.12(a,b)* and *Fig.A1(a,b))*, the ventricular pressure decreases, which means that the SBP decreases too, but the DBP increases, causing the reduction of the pulse pressure (SBP minus DBP). Conversely, peak velocities of the aorta and pulmonary artery *(Fig.12(c,d)* and *Fig.A1(c,d))* increase, showing a shorter ET, and a temporal delay that causes the increase of IVCT. Regarding the DA velocity, by decreasing the value of C_{lungs} *(Fig.12(e))*, a more physiological waveform is obtained but it presents an oscillatory behavior. On the contrary, the DA velocity achieves a better range of values by increasing the value of the systemic circulation vascular bed peripheral compliance (C_s) *(Fig.A1(e))*. On the other hand, our results suggested that by increasing the value of R_p (both pulmonary and systemic circulation vascular bed resistances), the velocity profiles of the aorta and pulmonary artery suffer the same changes as with C_p *(Fig.A2(c,d)* and *Fig.A3(c,d))*. Inversely, the ventricular pressure and, consequently, SBP, both increase; as well as DBP, keeping constant the pulse pressure *(Fig.A2(a,b)* and *Fig.A3(a,b))*. With respect to the DA velocity *(Fig.A2(e)* and *Fig.A3(e))*, it is considerably modified by varying the value of R_p, though it does not achieve a physiological waveform.

6.1.2) Ventricular activation timings

Figure 13 shows the two resulting plots of the parametric study on ventricular activation timings in healthy conditions: duration of the ventricular contraction and delay between atrial and ventricular contraction (*k* is the changing factor that multiplies the parameter's nominal value). The resulting plots of the elastance curve, the model-based pressure waveforms and the model-based velocity waveforms as a function of T_v and $delay$ are presented in Appendix B.

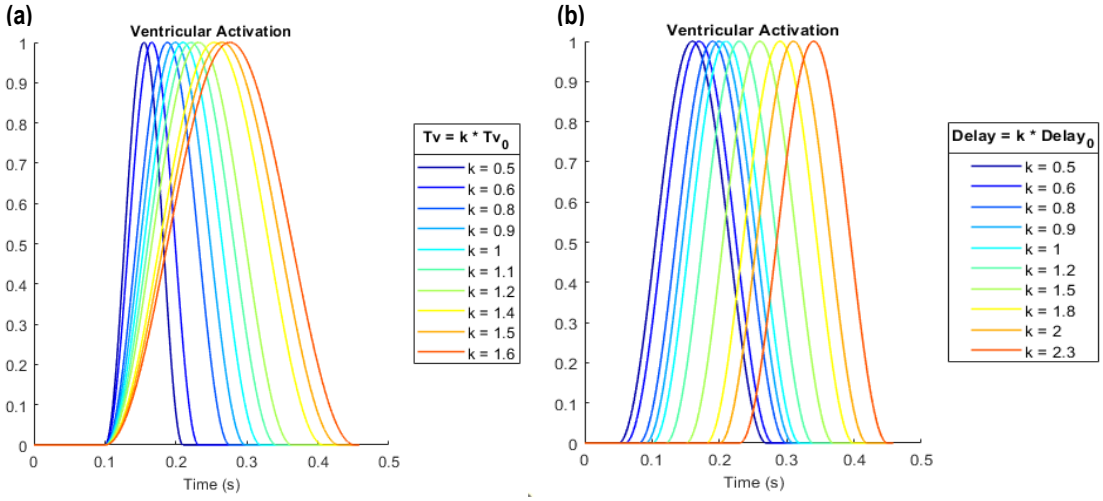

Figure 13. Model-based ventricular activation waveform resulting from the parametric study on the variation of: a) ventricular contraction duration (T_v); b) delay between atrial and ventricular contraction ($delay$)

The obtained results suggested that by increasing the value of T_v, the ventricular activation waveform *(Fig.13(a))* widens as expected, as well as the elastance curve *(Fig.B1(a))*, which causes pressure waveforms of ventricles and arteries *(Fig.B2(a,b))* to widen and decrease. Then, SBP decreases as well, whereas DBP increases, making the pulse pressure to decrease. Besides, it causes velocity waveforms of aorta and pulmonary artery *(Fig.B2(c,d))* to widen, meaning a longer ET, and to have a temporal delay, which means a longer IVCT. Their peak

velocities decrease. As for the DA velocity *(Fig.B2(e))*, it takes fewer negative values by increasing T_v. On the other hand, by increasing the value of $delay$, both the ventricular activation *(Fig.13(b))* and elastance *(Fig.B1(b))* curves are shifted to the right, which makes all model-based pressure *(Fig.B3(a,b))* and velocity waveforms *(Fig.B3(c,d,e))* to shift to the right as well. Thus, SBP and DBP do not change, and IVCT and ET become positive.

6.1.3) Diameters of mitral and tricuspid valves

Finally, *Figure 14* shows the model-based pressure and velocity waveforms from the single parametric study on the variation of the mitral valve diameter (*k* is the changing factor that multiplies the parameter's nominal value). The resulting plots showing the variation of the tricuspid valve diameter are presented in Appendix C.

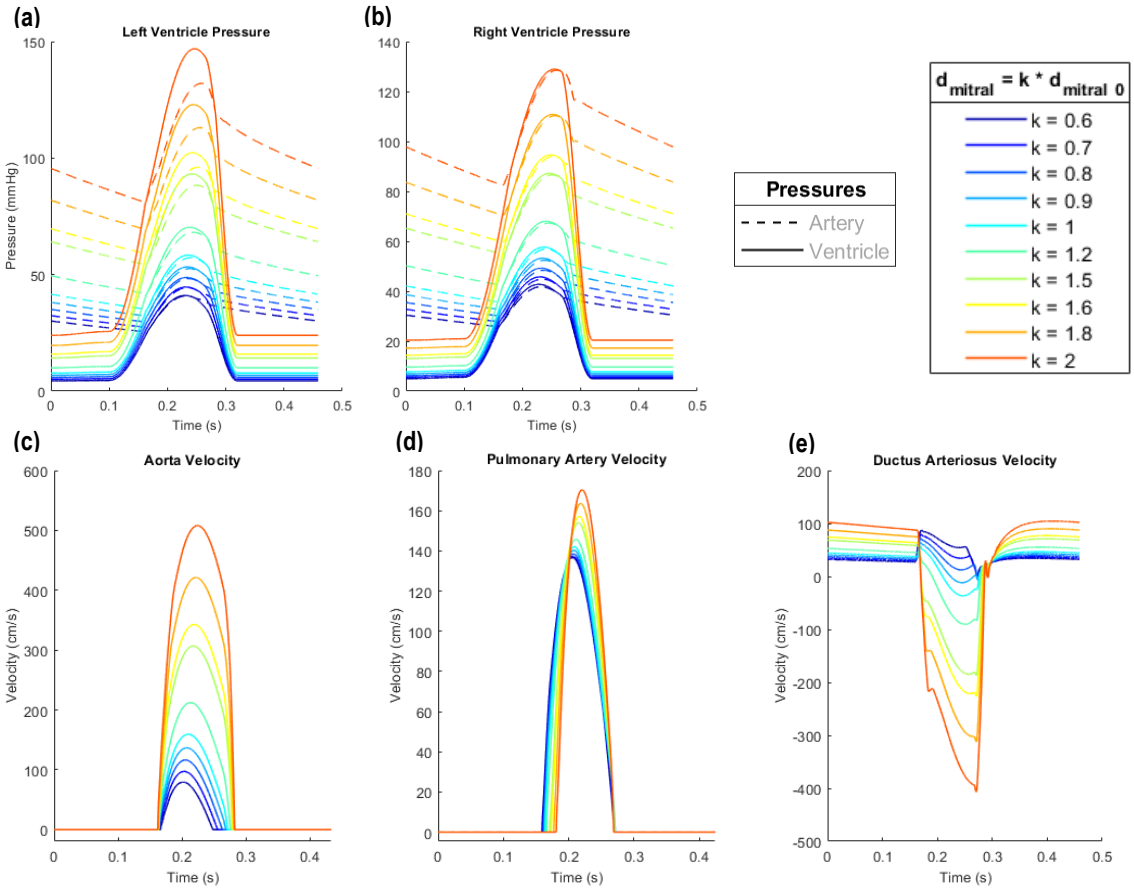

Figure 14. Model-based waveforms resulting from the parametric study on the variation of the mitral valve diameter: a) left ventricle and aorta pressure; b) right ventricle and pulmonary artery pressure; c) aorta velocity; d) pulmonary artery velocity; e) DA velocity

The obtained results suggested that by increasing the value of both diameters, pressures of left and right ventricles *(Fig.14(a,b)* and *Fig.C1(a,b))*, and velocity profiles of aorta and pulmonary artery *(Fig.14(c,d)* and *Fig.C1(c,d))* increase, reaching non-physiological values. The main difference between the variation that cause mitral and tricuspid diameters is the fact that the increase of the first one generates a greater change in the aorta velocity rather than in the pulmonary artery velocity, and vice versa. Concerning the DA velocity, by decreasing the mitral diameter *(Fig.14(e))*, it takes fewer negative values, as well as by increasing the value of the tricuspid diameter *(Fig.C1(e))*, although the waveforms obtained are not physiological.

To summarize, these parametric analyses have proven that the implemented model configuration of the fetal heart is able to reproduce the blood flow velocities and pressures in healthy conditions, but the values of the 8 selected parameters must be calibrated in order to obtain realistic waveforms and values. It must be mentioned that the DA is the one that suffers more drastic changes in its velocity profile that do not correspond to the measured waveform when modifying the value of the different model parameters.

6.2) Calibration of the simplified model of the fetal heart in healthy conditions

The result of the fetal heart 0D lumped model calibration is presented in this section. *Table 9* displays the calibrated values of the model parameters obtained after running the optimization algorithm. Then, *Figure 15* shows the model-based waveforms of the pressures in the left and right ventricles and arteries, and *Figure 16* shows the measured (dashed black line) and the model-based (solid blue line) waveforms of the velocity profiles of the aorta, pulmonary artery and DA. Besides, *Figure 17* presents the simulated cardiac timings, which correspond to the time intervals between the valves opening/closing. The measured and simulated values of the cardiac timings (FT, IVCT, ET and IVRT) and blood pressures (SBP, DBP and MBP), as described in section 5.4, are presented in *Table 10*, next to their relative error.

Table 9. Initial and final values after calibration of the fetal heart 0D lumped model

PARAMETER	VALUE	
	Initial	Calibrated
R_{lungs} (mmHg·s/ml)	36.2369	55.1042
C_{lungs} (ml/mmHg)	0.0516	0.0260
R_s (mmHg·s/ml)	4.0677	3.7320
C_s (ml/mmHg)	0.0935	0.1827
T_v (seconds)	0.22	0.319
$delay$ (seconds)	0.1	0.139
d_{mitral} (mm)	8.33	8.19
$d_{tricuspid}$ (mm)	8.61	8.08

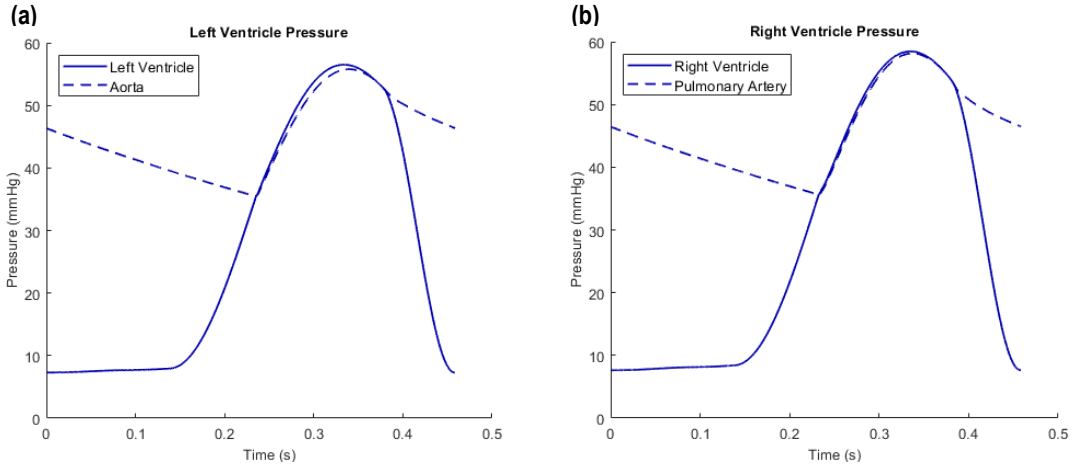

Figure 15. Model-based pressure waveforms of a) left ventricle and aorta, and b) right ventricle and pulmonary artery; after calibration of the fetal heart 0D lumped model

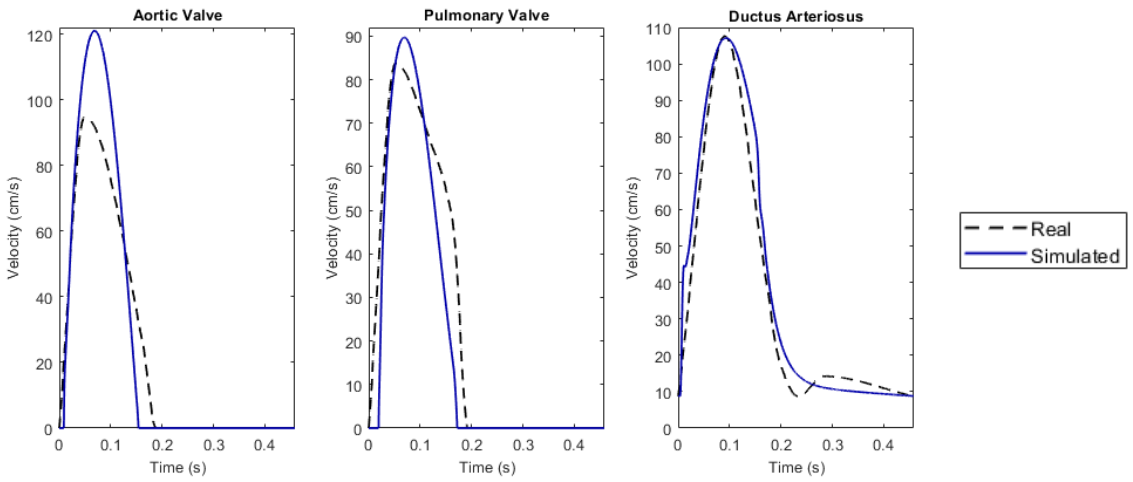

Figure 16. Measured and model-based velocity profiles of a) aortic valve, b) main pulmonary valve, and c) DA; after calibration of the fetal heart 0D lumped model

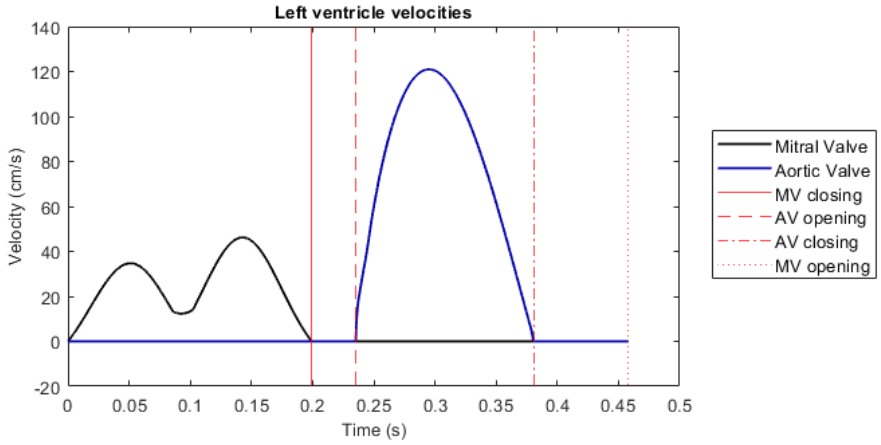

Figure 17. Model-based velocity profiles of mitral and aortic valves, highlighting the different cardiac events of mitral and aortic valves opening/closing, which designate the four cardiac timings (from left to right): FT, IVCT, ET, IVRT (MV: mitral valve, AV: aortic valve)

Table 10. Measured and modeled values after calibration of the fetal heart 0D lumped model, and its relative error

PARAMETER	VALUE		Relative error
	Real	Simulated	
FT (ms)	0.20	0.199	0.0005
IVCT (ms)	0.035	0.036	0.0305
ET (ms)	0.204	0.145	0.2877
IVRT (ms)	0.02	0.078	2.8523
SBP (mmHg)	52.70	55.96	0.0617
DBP (mmHg)	25.73	35.47	0.3788
MBP (mmHg)	40.53	42.30	0.0437
Aortic valve velocity	-	-	0.1279
Pulmonary valve velocity	-	-	0.1304
DA velocity	-	-	0.0703

The objective function, denoted by *J*, computed after executing the optimization algorithm described in section 5.4, which calculates the relative error between the model-based and the

real parameters, is 0.1257. This result state that the calibration process has been properly accomplished, since physiological model-based waveforms are achieved. Furthermore, the simulated values depicted in *Table 10* correspond roughly to the real ones, showing a small relative error. Therefore, the measured Doppler waveforms of a fetus in healthy conditions could be reproduced using the designed model. The rest of the final plots of ventricular flow, ventricular pressure-volume relationship, and velocity profiles are presented in Appendix D.

6.3) Evaluation of hemodynamic changes of cardiac defects in fetal circulation

6.3.1) VSD size

The main pathophysiologic mechanism of VSD is the shunt creation between the right and left ventricles [69]. In ToF, the shunted blood usually flows from the right side to the left one owing to the pulmonary obstruction (RVOTO) and higher pressure in the right ventricle, which causes poorly oxygenated blood to enter the systemic circulation where it mixes with oxygen-rich blood [14]. As described in section 5.5, the effects of VSD on the fetal hemodynamics have been assessed by defining a range of values that correspond to the VSD diameter. Therefore, in *Figure 18,* the changes occurring in the left and right ventricles' blood flow as a function of VSD size are shown. These results show that, as the VSD diameter increases which, consequently, causes the resistance that models this defect to decrease, the blood flow in the right ventricle decreases, while the blood flow in the left one increases, due to a higher pressure in the right ventricle. Thus, it allows to mimic the right-to-left shunt that occurs in ToF, which causes the overloading of the left ventricle volume and, subsequently, the reduction of the pulmonary circulation blood flow.

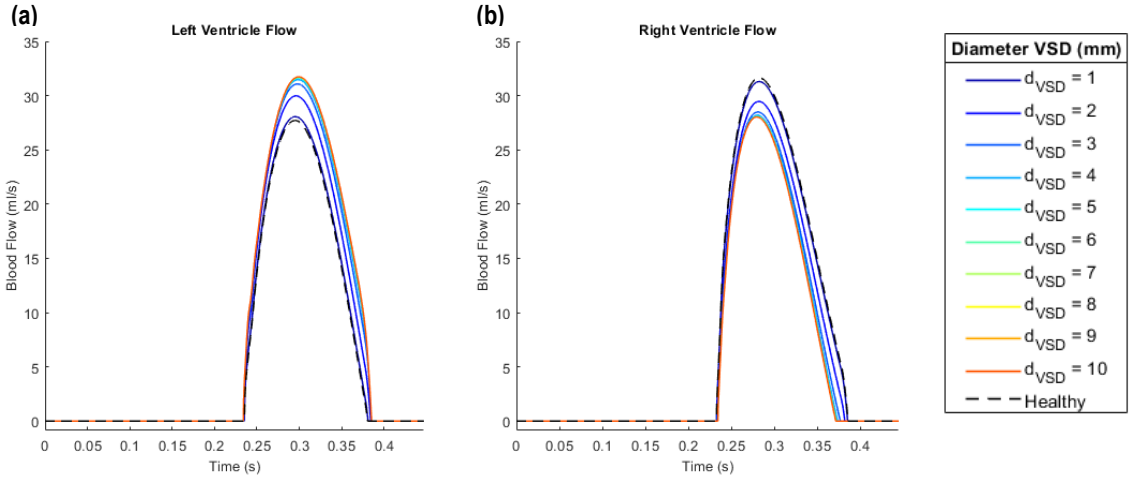

Figure 18. Model-based blood flow in a) left and b) right ventricles; when there is VSD in the fetal heart

In healthy conditions, there is no significant difference between left and right ventricular pressures of the human fetus [70], thus it is assumed that both ventricles operate at similar systemic pressures [71]. However, due to the presence of the VSD, the two ventricles can communicate in order to equalize their pressures, which was described by Wiputra et al. in 2018 [72]. Our results suggested this physiologic mechanism, as shown in *Figure 19*, so the right ventricle pressure slightly decreases, while the left one slightly increases in order to reach similar pressures, though the first one is always higher than the second one.

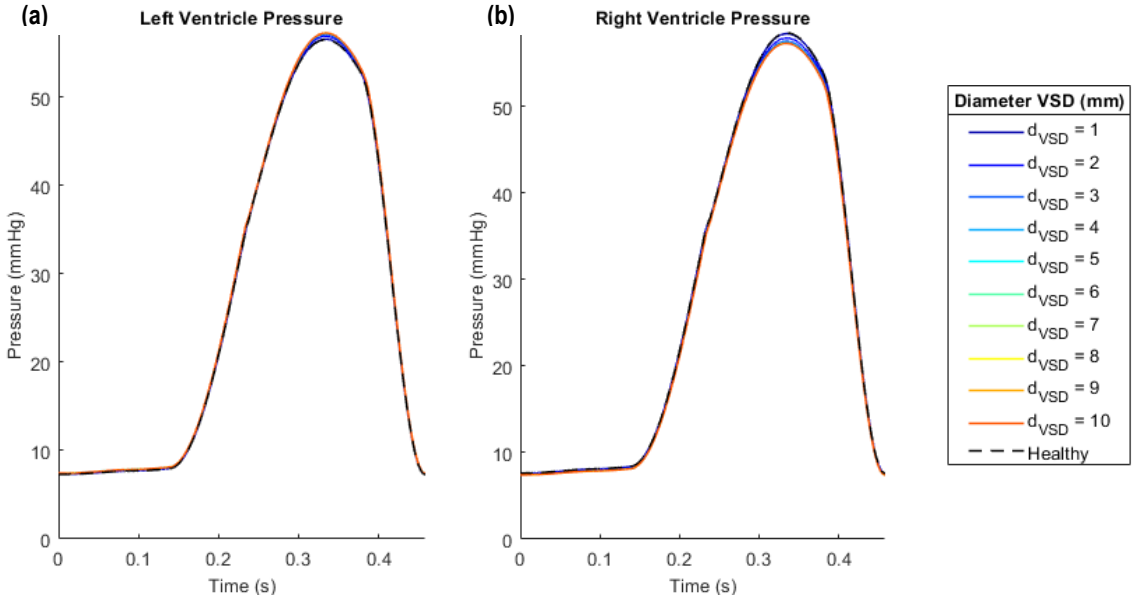

Figure 19. Model-based pressure in a) left and b) right ventricles; when there is VSD in the fetal heart

6.3.2) PVS degree

In ToF, severe PVS is caused by the reduction of the pulmonary valve diameter, leading to the obstruction of blood flow from the right ventricle to the pulmonary artery, which causes the right-to-left shunt through the VSD [14]. Therefore, since the pulmonary outflow resistance is increased, ToF ventricles require more work done for systolic ejection [72]. The effects of PVS degree in fetal hemodynamics have been modeled by decreasing the pulmonary valve diameter which, consequently, causes the dissipative coefficient of the pulmonary valve's non-linear resistor to increase. As described in section 5.5, quantitative evaluation of PVS severity is mainly based on the pressure gradient and the velocity profile across the pulmonary valve. Therefore, *Table 11* and *Figure 20* show the effects of PVS on pulmonary pressure gradient and velocity, respectively. These results suggested that the 0D lumped model makes an appropriate performance of the changes occurring in a ToF heart because, as the diameter of the cardiac valve decreases (increase of the valve stenosis), the pressure gradient increases, as well as the peak velocity in the pulmonary artery.

Table 11. Pressure gradient across the pulmonary valve when there is PVS in the fetal heart

Pulmonary valve diameter (mm)	Pressure gradient (mmHg)
6.7 *(Control healthy patient)*	3.22
6.03	4.79
5.36	7.37
4.69	11.78
4.02	19.63
3.35	34.56
2.68	67.03
2.01	158.52
1.34	538.95

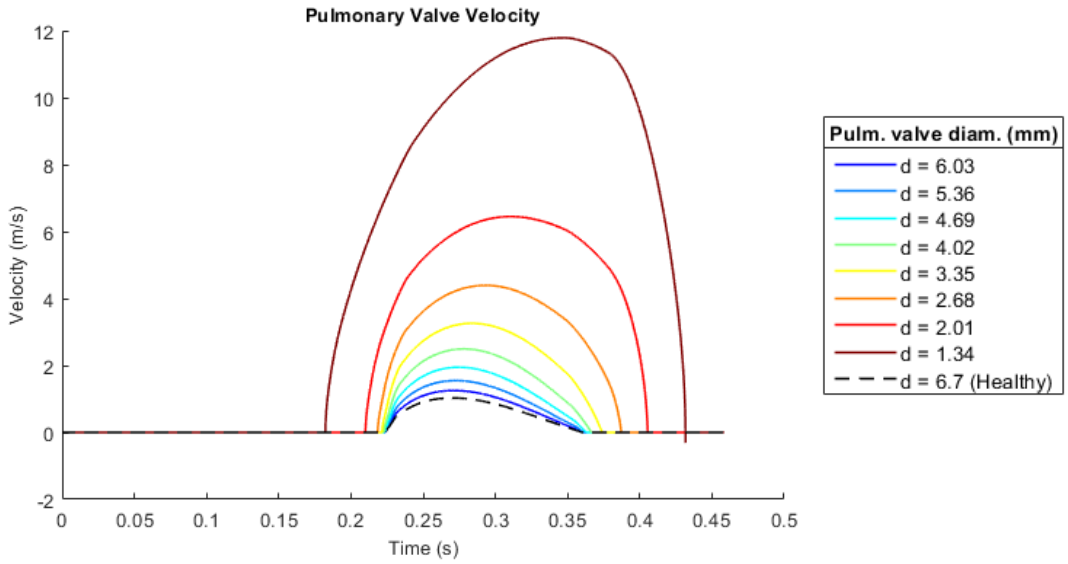

Figure 20. Model-based velocity profile in the pulmonary artery when there is PVS in the fetal heart

As discussed previously, PVS makes the pulmonary valve smaller, thus making harder for blood to flow out of the right ventricle into the pulmonary artery. Consequently, as the right ventricle tries to push blood through the valve, its pressure increases, which can eventually cause its hypertrophy (RVH) [14]. The increase of the right ventricular pressure as a consequence of the decrease of pulmonary valve diameter was also observed, as shown in *Figure 21(a)*. On the other hand, it has been stated that RVOTO enables to keep pulmonary artery pressure normal or below normal [73], which accounts for the increase in the transpulmonary pressure gradient discussed above. Therefore, this has been observed as well, as illustrated in *Figure 21(b)*.

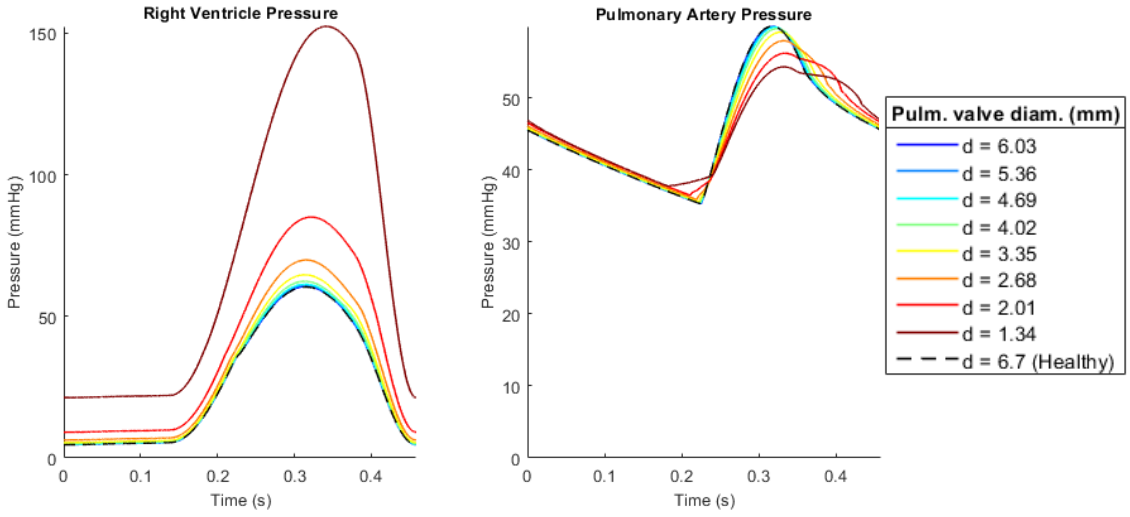

Figure 21. Model-based pressure when there is PVS in the fetal heart in: a) Right ventricle, b) Pulmonary artery

Furthermore, in *Figure 22(a)*, the relationship between pressure and volume in the right ventricle was plotted. What is important to mention here is the fact that, as blood finds harder to flow out of the right ventricle, its pressure increases but the volume does not change, that is the total right ventricular blood outflow remains constant. *Figure 22(b)* shows this pathophysiologic mechanism,

in which it can be seen that the maximum pulmonary artery blood flow decreases as the PVS degree increases but the velocity profile widens, thus confirming that it takes more time for blood to flow out of the right ventricle through the pulmonary valve.

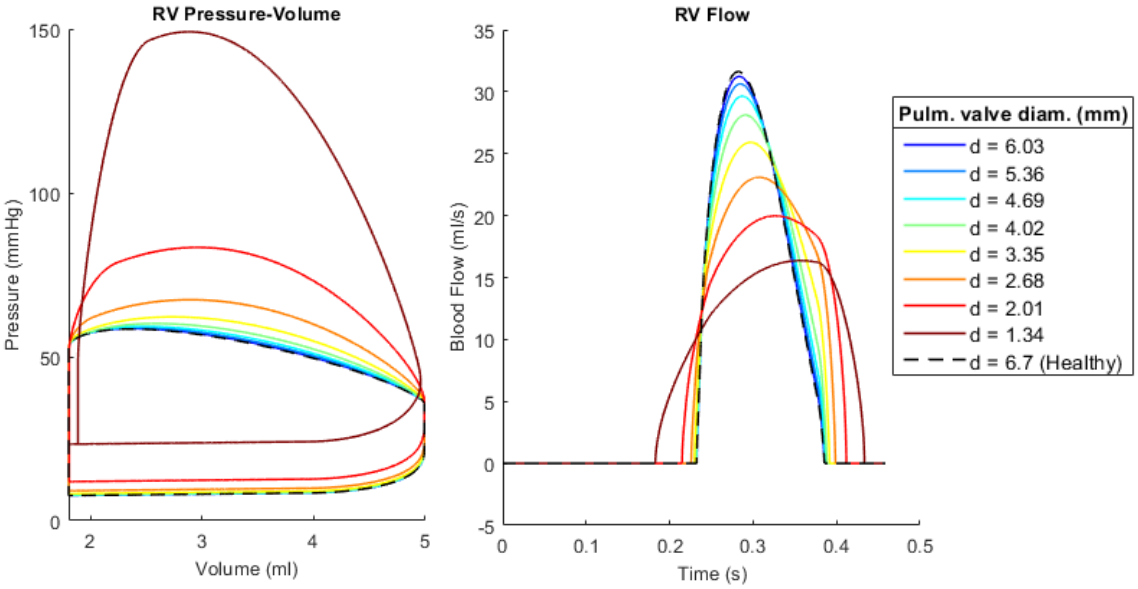

Figure 22. Model-based waveforms in the right ventricle when there is PVS in the fetal heart: a) Ventricular pressure-volume relationship, b) Ventricle blood flow (RV: right ventricle)

7) EXECUTION SCHEDULE

In this section, all tasks required for the development of the project as well as the time that was dedicated for each one are described. In order to see it in an organized and easy-understanding way, we used different methods, such as Work Breakdown Structure (WBS) and Gantt diagrams.

7.1) Tasks and time definition – WBS

WBS is a very important step for the execution of any project. Its objective is to define every task that is required for the study by stacking them in subgroups and making the organization of the project easier. In *Figure 23*, the WBS of our project is represented.

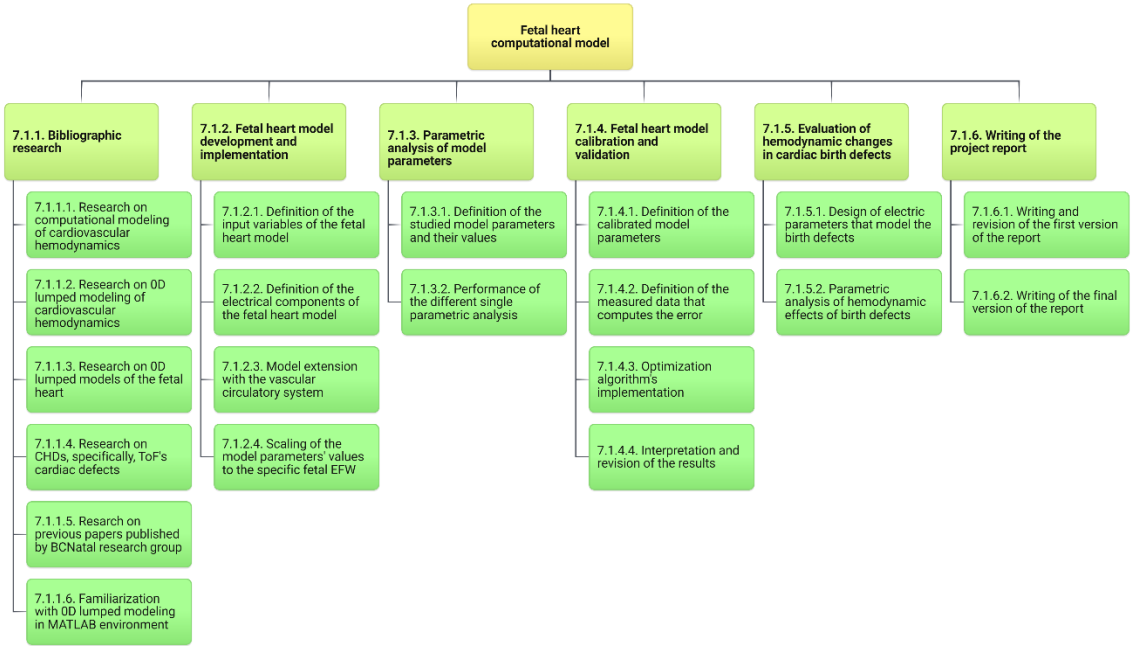

Figure 23. WBS of the project development

Next, a brief explanation of each of the tasks defined in the WBS is presented, along with the definition of the time required to execute each one. Finally, the total hours dedicated to each phase is shown in *Table 12*.

7.1.1) Bibliographic research

7.1.1.1) Research on computational modeling of cardiovascular hemodynamics (2 weeks)

The first step consisted in bibliographic research and analysis of the existent computational modeling techniques of cardiovascular dynamics, following the understanding of the difference between their dimensionalities. The importance of computational modeling in cardiovascular pathologies was comprehended.

7.1.1.2) Research on 0D lumped modeling of cardiovascular hemodynamics (3 weeks)

Then, bibliographic research and analysis of the 0D lumped parameter models was done, in order to understand the existent analogy between arterial system variables and electric

circuit components which are addressed a physiological meaning. The mathematical expressions and relationships of the 0D lumped model were defined.

7.1.1.3) Research on 0D lumped models of the fetal heart (3 weeks)

Bibliographic research and analysis of the existent fetal heart 0D lumped parameter models were done. Then, the different components the model includes, and the model parameters and values these require were described.

7.1.1.4) Research on CHDs, specifically, ToF's cardiac defects (2 weeks)

Finally, we reviewed the main features of CHDs affecting fetuses worldwide and their influence in the fetal circulation. Then, the hemodynamic changes occurring in ToF hearts were analyzed, and we searched information of the four basic cardiac defects this condition causes.

7.1.1.5) Research on previous papers published by BCNatal research group (3 weeks)

The already existent 0D lumped models implemented by BCNatal research group were analyzed, in order to extract the most important information and data to use it to develop our final fetal heart model.

7.1.1.6) Familiarization with 0D lumped modeling in MATLAB environment (4 weeks)

To finish this stage, we familiarized, understood, and trained with 0D lumped models using Simulink, MATLAB, in order to design, implement and simulate the different electrical circuits that define the compartments in fetal circulation, such as arterial segments and vascular beds.

7.1.2) <u>Fetal heart model development and implementation</u>

7.1.2.1) Definition of the input variables of the fetal heart model (4 weeks)

In this stage, first we specified the variables that constitute the fetal ventricles' inputs in healthy conditions, for the patient's specific GA. These include the blood velocity of the atrioventricular (both mitral and tricuspid) valves, the isovolumic pressure generator and the elastance functions.

7.1.2.2) Definition of the electrical components of the fetal heart model (4 weeks)

Then, we specified the components that compose the fetal heart, such as linear and non-linear resistances, compliances, and a diode for the valves. This step required much attention and time due to the difficulty of reproducing the opening and closing of the valves, which generate a characteristic pressure waveform on the aorta and pulmonary artery. At the end, we integrated the different block diagrams of the fetal heart.

7.1.2.3) Model extension with the vascular circulatory system (4 weeks)

We defined the block diagrams that are included in the simplified version of the vascular circulation which were finally added to our previous fetal heart model. Then, the values of the included model parameters were specified.

7.1.2.4) Scaling of the model parameters' values to the specific fetal EFW (2 weeks)

Finally, some of the hemodynamic parameters included in the 0D lumped model were scaled considering the EFW of the specific studied fetus, and using previously published allometric equations.

7.1.3) Parametric analysis of model parameters

7.1.3.1) Definition of the studied model parameters and their values (3 weeks)

The third phase started with an analysis of the parameters of the 0D lumped model of the fetal heart and circulation, and with the following specification of those parameters that have major relative importance on the model output.

7.1.3.2) Performance of the different single parametric analysis (5 weeks)

Lastly, the ranges of possible values of the chosen model parameters were defined, and their contribution on the model output was quantified. At the end, plots for each studied parameter were generated in order to enable its interpretation.

7.1.4) Fetal heart model calibration and validation

7.1.4.1) Definition of the calibrated model parameters (1 week)

In the fourth stage of the project, first we specified the set of model parameters that required to be calibrated in order to guarantee the fitting between the model-based outcomes and the patient-specific measurements.

7.1.4.2) Definition of the measured data that computes the error (1 week)

Then, the clinical and Doppler data from the healthy control fetus that enables the adjustment of the model parameters to fit the computational outputs was also specified.

7.1.4.3) Optimization algorithm's implementation (6 weeks)

The 0D lumped model of the fetal heart in healthy conditions was then calibrated, using an automatic optimization-based algorithm that was implemented in MATLAB, and which returned the values of the previously chosen set of model parameters that better fitted the model-based outcomes with the patient-specific data.

7.1.4.4) Interpretation and revision of the results (6 weeks)

Finally, revision and interpretation of the resulting plots and outcome values were done, following the correction of any parameter value required for the optimization process that might have caused large errors between the simulated outcomes and the real data.

7.1.5) Evaluation of hemodynamic changes in cardiac defects

7.1.5.1) Design of electric parameters that model the birth defects (2 weeks)

The penultimate phase started with the design and development in MATLAB, Simulink, of the fetal heart model that included two of the birth defects occurring in ToF: VSD and PVS. As for the VSD, a new 0D lumped model was implemented including an additional

resistance, whereas with respect to PVS, the model in healthy conditions was used but modifying a parameter value.

7.1.5.2) Parametric analysis of hemodynamic effects of birth defects (3 weeks)

To conclude with this stage, the effects that the size of VSD and the grade of PVS cause to the hemodynamics in fetal circulation were estimated. Then, the simulated outcomes were interpreted, and it was observed these could be extrapolated to real cases.

7.1.6) Writing of the project report

7.1.6.1) Writing and revision of the first version of the report (10 weeks)

The last stage of the project consisted in the writing of the project memory in order to describe its whole development. Then, different versions were reviewed and we corrected various mistakes.

7.1.6.2) Writing of the final version of the report (4 weeks)

To finish with the execution schedule, final writing of the project memory was performed, in which it was important to take into consideration the previous revisions and corrections.

To summarize, the total amount of time that each of the six phases required to do this project is presented in the following table:

Table 12. Summary of the total amount of hours required for the project development

MAIN TASKS	TOTAL DURATION (weeks)
Bibliographic research	7
Fetal heart 0D lumped model implementation	8
Parametric analysis of model parameters	8
Fetal heart model calibration and validation	9
Evaluation of hemodynamic changes in ToF's birth defects	4
Writing of the project report	13

7.2) Timing. Phases and milestones – Gantt diagram

Gantt chart represents the time duration of the phases and activities defined in the WBS. Its main goal is to do a chronological analysis of the different tasks and schedule the project timings. *Figure 24* shows the Gantt diagram of our project. As it can be observed, it starts in January 2021 and finishes in January 2022, excluding both months of July and August. Thus, the project has lasted a total of 11 months, as shown in the figure below, dedicating 400 hours approximately. To conclude with this section, the six milestones that have been assigned along the evolution of the project development are placed at the end of each phase.

Stage	Task	Jan. 2021	Feb. 2021	Mar. 2021	Apr. 2021	May 2021	June 2021	Sept. 2021	Oct. 2021	Nov. 2021	Dec. 2021	Jan. 2022
1	7.1.1.1 7.1.1.2 7.1.1.3 7.1.1.4 7.1.1.5 7.1.1.6											
2	7.1.2.1 7.1.2.2 7.1.2.3 7.1.2.4											
3	7.1.3.1 7.1.3.2											
4	7.1.4.1 7.1.4.2 7.1.4.3 7.1.4.4											
5	7.1.5.1 7.1.5.2											
6	7.1.6.1 7.1.6.2											

Figure 24. Gantt diagram of the final degree project

8) TECHNICAL VIABILITY

In this section, a SWOT analysis is going to be examined, which is a strategic planning technique that allows the identification of the internal factors of the environment (strengths and weaknesses) as well as the external ones (opportunities and threats) that might affect the realization of the project, both positively and negatively. In this case, this analysis will be focused mostly on the decision of using a 0D lumped parameter model in order to simulate the hemodynamics of the fetal heart, and enable the estimation of the effects occurring in ToF disease.

8.1) SWOT analysis

In *Table 13*, there is a summary of the strengths, weaknesses, opportunities and threats that have been extracted from this final degree project, so that it can give an overview of the workflow that it has followed and help to identify which aspects have helped in its development and which have not.

Table 13. SWOT analysis of the project

	Positive factors	**Negative factors**
Internal environment	**STRENGHTS**	**WEAKNESSES**
	- Performance of patient-specific simulations in order to validate the fetal heart model. - Collaboration with different important institutions, such as Hospital Clínic de Barcelona. - Ease physician's work in understanding of hemodynamic changes occurring in ToF. - Enable to extract data and information from previous studies of the same research group.	- Lack of accuracy in the computational outcomes. Model-based waveforms do not exactly reproduce the measured data. - More control patients in healthy conditions could have been used to validate the model. - Only two birth defects in ToF have been evaluated, and the model just accounts for the isolated birth defects without considering the simultaneity of all of them.
External environment	**OPPORTUNITIES**	**THREATS**
	- 0D lumped parameter model is a promising tool for the study and management of fetal cardiovascular disorders. - It is the first model of the fetal heart that specifically studies ToF hemodynamic changes. - It can contribute to development of novel fetal interventional strategies.	- 0D lumped parameter models do not include multi-dimensional flow effects. - There is limited published data on blood flow mechanics in fetal ToF and on remodeling of the disease. - More model parameters are required to be studied and corrected in order to understand the mechanism of the model.

9) ECONOMIC VIABILITY

This section includes the estimation of all costs that are required for the development of this final degree project. It is useful in order to increase the probability of success of the project by detecting the different tasks that may affect and be prejudicial to its final results, as well as it enables to notice any sign that may suggest that it is better to change some of the required tasks. Therefore, we are going to first talk about the approximated economical budget of the project taking into consideration the resources that are needed and then, we are going to expose the cost relating to the devices, personnel, and dedicated hours.

9.1) Estimation and analysis of costs and budgets

The total economic costs of the project include the cost of developing the 0D lumped parameter model, which consists in the necessary equipment, and the salary of the workers. In *Table 14*, the material and the workers required to develop the project are reviewed.

Regarding the required material to develop this project, it includes both software and hardware. The software needed is MATLAB and Simulink (2019b, The MathWorks Inc., Natick, MA). It is necessary to purchase a license in order to use it, and there are different licenses depending on its final use. Since this project has been developed as part of the bachelor's degree, it has educational and academic research purposes. Therefore, we have used the student license that is intended for teachers and students at a degree-granting institution, such as Universitat de Barcelona, and that includes MATLAB, Simulink, and 10 of the most widely used add-on products for control systems, signal and image processing, statistics, optimization, and symbolic math. Its price is listed in *Table 14*, which is assumed by the Universitat de Barcelona.

On the other hand, the hardware used in this final degree project is a computer that enables to download the software, develop the whole 0D lumped model, and perform the different simulations. A personal laptop has been used in this project, the estimated cost of which ranges from 500 to 5000 €, and it is also listed in *Table 14*. In addition, medical equipment from the hospital is required in order to collect the data from patients. Specifically, Doppler ultrasound has been used on different pregnant women, and the results have been provided by Hospital Clínic de Barcelona. The price of an ultrasound device is not much expensive, and it can vary from 20000 to 65000 €.

Concerning the expenses due to the technical staff working on this project, this consists in a biomedical engineering student, the project's supervisor, and the project's director, as defined in *Table 14*. The student is considered as a junior or beginner engineer, whose salary is approximately 15 €/h. As defined in section 7.2, this project has taken 400 hours. The supervisor of the project is a postdoctoral researcher and engineer, and the director is a fetal cardiologist in Hospital Clínic de Barcelona, both being part of BCNatal-FMRC. Their salary is estimated to be 25 €/h and the dedicated hours have been 50 and 10, respectively.

As for the facilities that we have used during this project, this is just Hospital Clínic de Barcelona, from which the clinical and Doppler data has been extracted. The rest of the project has been performed remotely due to COVID-19 pandemic. Therefore, this does not present any additional cost to the final budget estimation.

Table 14. Summary of total costs of this final degree project

Item	Units	Unit cost	Total cost
MATLAB Student License	1	69 €	69 €
Personal laptop	1	1.500 €	1.500 €
Doppler ultrasound	1	65.000 €	65.000 €
Biomedical engineering student	1	15 €/h	6.000 €
Project's supervisor	1	25 €/h	1.250 €
Project's director	1	25 €/h	250 €
TOTAL			**74.069 €**

10) REGULATORY AND LEGAL ASPECTS

In this section, different laws that are applicable to this final degree project, and to the acquisition of clinical personal data, are going to be displayed. There will be discussed some of the regulations from Spain and European Union regulations, as well as there are some international standards presented.

10.1) Applicable law: norms and regulations

First, the developed fetal heart 0D lumped parameter model requires clinical data from patients of Hospital Clínic de Barcelona for its design and validation. Therefore, it is important to keep patient privacy regulations up to date. In Spain, AEPD *(Agencia Española de Protección de Datos)* is the agency responsible for the compliance with data protection regulations in the treatment of health data. LOPDGDD *(Ley Orgánica de Protección de Datos y de Garantía de Derechos Digitales)* refers to the organic law of data protection in Spain, which was approved in December 2018, that determines the requirements of the companies that have to manipulate personal information such as text, images or audio data. The goal of this law is to protect the individual privacy and confidentiality and to regulate the processes of data transfer so as to guarantee their security [74]. Thus, the clinical data from pregnant women that was used in this project was anonymized.

Concerning the acquisition of data using Doppler ultrasound, there are some standards in Spain for the use of ultrasound scanners, which are diagnostic medical equipment belonging to class II, meaning that they present a small degree of invasiveness and risk to the patient. The standards include UNE-EN 61157:2007, which regards the standard means for the reporting of the acoustic emissions of medical diagnostic ultrasonic equipment [75]; and UNE-EN 61266:1996, which presents the requirements for the performance of Doppler ultrasounds when detecting the fetal heartbeat [76]. At the European Union level, any medical device must comply with the CE marking, which is a mandatory certification given by the public administration that states that a product meets with the regulatory technical requirements to permit its commercialization. In this case, ultrasound equipment that was used to acquire the clinical data from Hospital Clínic de Barcelona respect those regulations and CE marking.

Finally, ISOs (International Organization for Standardization) are international standards that ensure the quality, safety and efficiency of products. ISO 9001 (Quality certification) specifies the requirements that any company must comply so that there is a proper quality administration of the product that guarantees its efficiency and optimal service to clients [77]. Specifically in the case of ultrasounds, ISO 13379-1:2012 (Condition monitoring and diagnostics of machines – Data interpretation and diagnostics techniques) states the guidelines for the procedures that have to determine the condition of ultrasound scanners. Thus, these methods might advise when there is an anomalous behavior that may harm the outcomes [78].

11) CONCLUSIONS AND FUTURE LINES

In this final degree project, we have designed and implemented a 0D lumped parameter model of the fetal heart in order to study the hemodynamic changes occurring in ToF disease, specifically, two of its four birth defects: VSD and PVS.

Regarding the development of the whole project, first we reviewed the already existent 0D lumped models of the fetal circulation, taking particular interest in the previous studies performed by Garcia-Cañadilla et al. in BCNatal research group for the vascular circulatory system, and in the published papers by Pennati et al. for the fetal heart. After designing the electrical components of the fetal heart, and extending the model with a simplified version of the vascular circulation, the nominal values of all the model parameters were assigned and we scaled them according to the EFW of the healthy control fetus. Then, different parametric analyses were performed in order to quantify the contribution of the different parameters on the model outcomes. As we have discussed in section 6.1, these results suggested that the selected model parameters must be calibrated in healthy conditions so as our 0D lumped model can reproduce the behavior of the fetal heart. Moreover, we saw that the velocity profile of DA did not have a physiological waveform, meaning that the parameters modeling this arterial segment should be better adjusted.

Then, the calibration of the proposed 0D lumped model in healthy conditions was performed so as to guarantee that the model simulations mimic the patient-specific measurements. A set of different parameters was calibrated using an optimization algorithm in MATLAB that gave the minimum possible error between the model-based and the real data. In this case, we saw that the model is able to reproduce the measured velocity profiles and blood pressures, with a total error, computed with the velocity profiles of aorta, main pulmonary artery and DA, and the values of the cardiac timings and blood pressures, of 0.1257.

Finally, once the model was validated and a good approximation to the real hemodynamics of the fetal heart was ensured, the birth defects of VSD and PVS were modeled and the effects these cause to the fetal circulation were analyzed. The resulting parametric analyses evaluating the VSD size show that its increase cause the blood flow in the right ventricle to decrease while in the left ventricle increases, which means that our model is enable to mimic the right-to-left shunt, characteristic in ToF condition. Moreover, we also evaluated the ventricular pressures and we saw that the VSD cause them to equalize. On the other hand, when evaluating the effect of PVS degree on fetal hemodynamics, we could conclude that our 0D lumped model has also been able to simulate the hemodynamic effects occurring in the fetal heart. As the PVS degree increases, we have seen that the pressure gradient across the pulmonary valve increases, going from mild (<36 mmHg) to severe stenosis (>64 mmHg), following the classification of PVS severity. Simultaneously, the peak velocity of the pulmonary artery increases. Further, we also proved that the RVOTO causes the right ventricular pressure to increase much because it makes harder for blood to flow out of the chamber. Finally, the behavior of blood flow inside the ventricle was also evaluated, confirming that it needs more time in order to flow out from the ventricle.

Nevertheless, this fetal heart model presents some limitations that are going to be discussed. Regarding the design of the model of just the fetal heart, it must be mentioned that only the ventricles and arterial valves were included, thus leaving out the atria and atrioventricular valves, since we used the mitral and tricuspid blood flow as input for the model. In future works, these should be modeled as well in order to simulate the fetal heart hemodynamics more realistically, and be able to simulate problems related with the atria and atrioventricular valves. As for the calibration of the model, it was performed just using data from a single healthy patient. We propose to perform a calibration to capture also individuals' variability as well as changes during gestation. Moreover, the calibration of the simplified model in healthy conditions was performed using the model-based velocity waveforms of the aorta, main pulmonary artery and DA, and the values of different cardiac variables, excluding the velocity profile of the pulmonary circulatory system, since real Doppler velocity data from the pulmonary circulation was not available. Although we have ensured that the model-based waveform of the pulmonary vascular bed reassemble the real velocity profile, it should be incorporated in the process in order to be more reliable. Regarding the nominal values that have been assigned to the cardiac parameters, these have been extracted from the literature or from previous projects of the same research group, for the specific GA of the healthy fetus. Ideally, these values should be generalized to be able to calculate them for any GA, like the equations that describe the physical dimensions of the vessels, so as to facilitate the study of any other fetus with different GA, and not just the one studied here. On the other hand, the 0D lumped models simulating some of the cardiac defects present in ToF have not been calibrated, which means that the accuracy and precision of the outcomes cannot be assured. Finally, regarding the modeling of VSD and PVS, a limitation of our 0D lumped model is that it just accounts for the isolated heart defects without considering them simultaneously.

Moreover, an important drawback considering the main aim of this project is the lack of literature and clinical data defining the different parameters of the fetal heart, as well as describing hemodynamic changes in fetuses with ToF. Therefore, knowledge of which could be very helpful in order to provide insight into the reliability of the final model-based outcomes extracted from the evaluation of the effects in hemodynamics of VSD and PVS.

In conclusion, we have seen that the 0D lumped model of the fetal heart developed in this project is able to reproduce the real blood flow in an accurate way, although there are some important limitations that should be analyzed in order to improve its outcomes. Regarding the ToF heart, we have proven that the model can suggest conclusive approximations to the estimation of the effects in hemodynamics of VSD and PVS. Based on this, it is essential to make future research continuing the results of this study.

BIBLIOGRAPHY

[1] Savoji, H., Mohammadi, M. H., Rafatian, N., Toroghi, M. K., Wang, E. Y., Zhao, Y., Korolj, A., Ahadian, S., & Radisic, M. (2019). Cardiovascular disease models: A game changing paradigm in drug discovery and screening. Biomaterials, 198, 3–26. https://doi.org/10.1016/j.biomaterials.2018.09.036

[2] Bragard, J. R., Camara, O., Echebarria, B., Gerardo Giorda, L., Pueyo, E., Saiz, J., Sebastián, R., Soudah, E., & Vázquez, M. (2021). Cardiac computational modelling. Revista española de cardiología (English ed.), 74(1), 65–71. https://doi.org/10.1016/j.rec.2020.05.024

[3] Shi, Y., Lawford, P., & Hose, R. (2011). Review of zero-D and 1-D models of blood flow in the cardiovascular system. Biomedical engineering online, 10, 33. https://doi.org/10.1186/1475-925X-10-33

[4] Bouma, B. J., & Mulder, B. J. (2017). Changing Landscape of Congenital Heart Disease. *Circulation research, 120*(6), 908–922. https://doi.org/10.1161/CIRCRESAHA.116.309302

[5] Wanni, K. A., Shahzad, N., Ashraf, M., Ahmed, K., Jan, M., & Rasool, S. (2014). Prevalence and spectrum of congenital heart diseases in children. *Heart India, 2*(3), 76.

[6] van der Bom, T., Zomer, A. C., Zwinderman, A. H., Meijboom, F. J., Bouma, B. J., & Mulder, B. J. (2011). The changing epidemiology of congenital heart disease. *Nature reviews. Cardiology, 8(*1), 50–60. https://doi.org/10.1038/nrcardio.2010.166

[7] Biglino, G., Capelli, C., Bruse, J., Bosi, G. M., Taylor, A. M., & Schievano, S. (2017). Computational modelling for congenital heart disease: how far are we from clinical translation?. Heart (British Cardiac Society), 103(2), 98–103. https://doi.org/10.1136/heartjnl-2016-310423

[8] Corsini, C., Baker, C., Kung, E., Schievano, S., Arbia, G., Baretta, A., Biglino, G., Migliavacca, F., Dubini, G., Pennati, G., Marsden, A., Vignon-Clementel, I., Taylor, A., Hsia, T. Y., Dorfman, A., & Modeling of Congenital Hearts Alliance (MOCHA) Investigators (2014). An integrated approach to patient-specific predictive modeling for single ventricle heart palliation. *Computer methods in biomechanics and biomedical engineering, 17*(14), 1572–1589. https://doi.org/10.1080/10255842.2012.758254

[9] [9] Biglino, G., Cosentino, D., Steeden, J. A., De Nova, L., Castelli, M., Ntsinjana, H., Pennati, G., Taylor, A. M., & Schievano, S. (2015). Using 4D Cardiovascular Magnetic Resonance Imaging to Validate Computational Fluid Dynamics: A Case Study. *Frontiers in pediatrics, 3*, 107. https://doi.org/10.3389/fped.2015.00107

[10] LaDisa, J. F., Jr, Alberto Figueroa, C., Vignon-Clementel, I. E., Kim, H. J., Xiao, N., Ellwein, L. M., Chan, F. P., Feinstein, J. A., & Taylor, C. A. (2011). Computational simulations for aortic coarctation: representative results from a sampling of patients. *Journal of biomechanical engineering, 133*(9), 091008. https://doi.org/10.1115/1.4004996

[11] Pérez-Lescure Picarzo, J., Mosquera González, M., Latasa Zamalloa, P., & Crespo Marcos, D. (2018). Mortalidad de las cardiopatías congénitas en España durante 10 años (2003-2012) [Congenital heart disease mortality in Spain during a 10 year period (2003-2012)]. *Anales de pediatria, 88*(5), 273–279. https://doi.org/10.1016/j.anpedi.2017.06.002

[12] Shimizu, S., Une, D., Kawada, T., Hayama, Y., Kamiya, A., Shishido, T., & Sugimachi, M. (2018). Lumped parameter model for hemodynamic simulation of congenital heart diseases. *The journal of physiological sciences: JPS, 68*(2),103-111. https://doi.org/10.1007/s12576-017-0585-1

[13] Wilson, R., Ross, O., & Griksaitis, M. J. (2019). Tetralogy of Fallot. *BJA education, 19*(11), 362–369. https://doi.org/10.1016/j.bjae.2019.07.003

[14] G. Ottaviani, L.M. Buja. (2016). Chapter 15 - Congenital Heart Disease: Pathology, Natural History, and Interventions, Editor(s): L. Maximilian Buja, Jagdish Butany, *Cardiovascular Pathology (Fourth Edition)* (pp. 611-647). Academic Press. ISBN 9780124202191. https://doi.org/10.1016/B978-0-12-420219-1.00014-8

[15] Wise-Faberowski, L., Asija, R., & McElhinney, D. B. (2019). Tetralogy of Fallot: Everything you wanted to know but were afraid to ask. *Paediatric anaesthesia, 29*(5), 475–482. https://doi.org/10.1111/pan.13569

[16] Hafen, B. B., & Sharma, S. (2021). Oxygen Saturation. In StatPearls. StatPearls Publishing. Accessed: December 2021

[17] Kokalari, I. , Karaja, T. and Guerrisi, M. (2013) Review on lumped parameter method for modeling the blood flow in systemic arteries. *Journal of Biomedical Science and Engineering*, 6, 92-99. doi: 10.4236/jbise.2013.61012

[18] Broomé, M., Maksuti, E., Bjällmark, A., Frenckner, B., & Janerot-Sjöberg, B. (2013). Closed-loop real-time simulation model of hemodynamics and oxygen transport in the cardiovascular system. *Biomedical engineering online, 12,* 69. https://doi.org/10.1186/1475-925X-12-69

[19] Marcela Szopos (2017). Mathematical modeling, analysis and simulations for fluid mechanics and their relevance to in silico medicine. Analysis of PDEs [math.AP]. Université de Strasbourg, IRMA UMR 7501. ⟨tel-01646867⟩

[20] Michel E. Safar, Bernard I. Lévy (2007), 'Chapter 13 - Resistance Vessels in Hypertension', Editor(s): Gregory Y.H. Lip, John E. Hall, *Comprehensive Hypertension*, Mosby, pp. 145-150

[21] Catanho, M.T., Sinha, M., & Vijayan, V. (2012). Model of Aortic Blood Flow Using the Windkessel Effect. *BENG 221 - Mathematical Methods in Bioengineering*.

[22] Westerhof, N., Stergiopulos, N., Noble, M. I. M. (2010). Snapshots of hemodynamics. An Aid for Clinical Research and Graduate Education. (Second Edition). *Springer US.*

[23] Milišić, V., & Quarteroni, A. (2004). Analysis of lumped parameter models for blood flow simulations and their relation with 1D models. *ESAIM: Mathematical Modelling and Numerical Analysis, 38*(4), pp. 613-632. https://doi:10.1051/m2an:2004036

[24] Blanco, P.J., & Feijóo, R.A. (2010). A 3D-1D-0D Computational Model for the Entire Cardiovascular System. Laboratório Nacional de Computação Científica LNCC/MCT.

[25] Gul, Raheem. (2016). Mathematical Modeling and Sensitivity Analysis of Lumped-Parameter Model of the Human Cardiovascular System. Dr. rer. nat. thesis. Freie Universität Berlin.

[26] Zhou, S., Xu, L., Hao, L., Xiao, H., Yao, Y., Qi, L., & Yao, Y. (2019). A review on low-dimensional physics-based models of systemic arteries: application to estimation of central aortic pressure. *Biomedical engineering online, 18*(1), 41. https://doi.org/10.1186/s12938-019-0660-3

[27] Formaggia, Luca & Veneziani, Alessandro. (2003). Reduced and multiscale models for the human cardiovascular system. Politecnico di Milano

[28] Pennati G, Bellotti M. (1995). Doppler waveforms of the human fetal cardiovascular system: a mathematical model. *WIT Transactions on Biomedicine and Health* vol 2. Politecnico di Milano, Italy

[29] Pennati, G., Bellotti, M., & Fumero, R. (1997). Mathematical modelling of the human foetal cardiovascular system based on Doppler ultrasound data. *Medical engineering & physics, 19*(4), 327–335. https://doi.org/10.1016/s1350-4533(97)84634-6

[30] Pennati, G., Migliavacca, F., Dubini, G., Pietrabissa, R., & de Leval, M. R. (1997). A mathematical model of circulation in the presence of the bidirectional cavopulmonary anastomosis in children with a univentricular heart. *Medical engineering & physics, 19*(3), 223–234. https://doi.org/10.1016/S1350-4533(96)00071-9

[31] Pennati, G., Migliavacca, F., Dubini, G., Pietrabissa, R., Fumero, R., & de Leval, M. R. (2000). Use of mathematical model to predict hemodynamics in cavopulmonary anastomosis with persistent forward flow. *The Journal of surgical research, 89*(1), 43–52. https://doi.org/10.1006/jsre.1999.5799

[32] Couto, P. M. S., van Meurs, W. L., Bernardes, J. F., de Sá, J. P. M., & Goodwin, J. A. (2002). Mathematical model for educational simulation of the oxygen delivery to the fetus. *Control Engineering Practice, 10*(1), 59-66.

[33] Huikeshoven, F. J., Hope, I. D., Power, G. G., Gilbert, R. D., & Longo, L. D. (1985). Mathematical model of fetal circulation and oxygen delivery. *American Journal of Physiology-Regulatory, Integrative and Comparative Physiology, 249*(2), R192-R202.

[34] van den Wijngaard, J. P., Westerhof, B. E., Faber, D. J., Ramsay, M. M., Westerhof, N., & Van Gemert, M. J. (2006). Abnormal arterial flows by a distributed model of the fetal circulation. *American Journal of Physiology-Regulatory, Integrative and Comparative Physiology, 291*(5), R1222-R1233.

[35] Myers, L. J., & Capper, W. L. (2002). A transmission line model of the human foetal circulatory system. *Medical engineering & physics, 24*(4), 285-294.

[36] Garcia-Canadilla, P., Rudenick, P. A., Crispi, F., Cruz-Lemini, M., Palau, G., Camara, O., Gratacos, E., & Bijnens, B. H. (2014). A computational model of the fetal circulation to quantify blood redistribution in intrauterine growth restriction. *PLoS computational biology, 10*(6), e1003667. https://doi.org/10.1371/journal.pcbi.1003667

[37] P. Garcia-Canadilla, et al., Patient-specific estimates of vascular and placental properties in growth-restricted fetuses based on a model of the fetal circulation, Placenta (2015), http://dx.doi.org/10.1016/j.placenta.2015.07.130

[38] Garcia-Canadilla P, Rudenick. P., Crispi, F., Cruz-Lemini, M., Palau, G., Gratacos, E., Bijnens, B. H. Understanding Prenatal Brain Sparing by Flow Redistribution Based on a Lumped Model of the Fetal

Circulation. Lecture Notes in Computer Science; 2013 June 20–22, 2013; London, UK. Springer Berlin Heidelberg. pp. 123–131

[39] Korurek, M., Yildiz, M., Yüksel, A., & Şahin, A. (2012). Simulation of Eisenmenger syndrome with ventricular septal defect using equivalent electronic system. *Cardiology in the young, 22*(3), 301–306. https://doi.org/10.1017/S1047951111001478

[40] Tang, H., Dai, Z., Wang, M. et al. Lumped-Parameter Circuit Platform for Simulating Typical Cases of Pulmonary Hypertensions from Point of Hemodynamics. *J. of Cardiovasc. Trans. Res.* 13, 826–852 (2020). https://doi.org/10.1007/s12265-020-09953-y

[41] Yigit, B., Tutsak, E., Yıldırım, C., Hutchon, D., & Pekkan, K. (2019). Transitional fetal hemodynamics and gas exchange in premature postpartum adaptation: immediate vs. delayed cord clamping. *Maternal health, neonatology and perinatology, 5*, 5. https://doi.org/10.1186/s40748-019-0100-1

[42] Pennati, G., Corsini, C., Hsia, T. Y., Migliavacca, F., & Modeling of Congenital Hearts Alliance (MOCHA) Investigators (2013). Computational fluid dynamics models and congenital heart diseases. *Frontiers in pediatrics, 1*, 4. https://doi.org/10.3389/fped.2013.00004

[43] Marsden, A. L., & Feinstein, J. A. (2015). Computational modeling and engineering in pediatric and congenital heart disease. Current opinion in pediatrics, 27(5), 587–596. https://doi.org/10.1097/MOP.0000000000000269

[44] AIUM Practice Parameter for the Performance of Fetal Echocardiography. (2020). *Journal of ultrasound in medicine : official journal of the American Institute of Ultrasound in Medicine, 39*(1), E5–E16. https://doi.org/10.1002/jum.15188

[45] Committee on Practice Bulletins—Obstetrics and the American Institute of Ultrasound in Medicine (2016). Practice Bulletin No. 175: Ultrasound in Pregnancy. *Obstetrics and gynecology, 128*(6), e241–e256. https://doi.org/10.1097/AOG.0000000000001815

[46] Allan L. (2004). Technique of fetal echocardiography. *Pediatric cardiology, 25*(3), 223–233. https://doi.org/10.1007/s00246-003-0588-y

[47] Papp, Z., & Fekete, T. (2003). The evolving role of ultrasound in obstetrics/gynecology practice. *International journal of gynaecology and obstetrics: the official organ of the International Federation of Gynaecology and Obstetrics, 82*(3), 339–346. https://doi.org/10.1016/s0020-7292(03)00224-8

[48] Gowda, R. M., Khan, I. A., Vasavada, B. C., Sacchi, T. J., & Patel, R. (2004). History of the evolution of echocardiography. *International journal of cardiology, 97*(1), 1–6. https://doi.org/10.1016/j.ijcard.2003.07.018

[49] Araujo Júnior, E., Nardozza, L. M., & Moron, A. F. (2013). Three-dimensional ultrasound STIC-HDlive rendering: new technique to assessing of fetal heart. *Revista brasileira de cirurgia cardiovascular : orgao oficial da Sociedade Brasileira de Cirurgia Cardiovascular, 28*(4), v–vii. https://doi.org/10.5935/1678-9741.20130070

[50] Gray, R. A., & Pathmanathan, P. (2018). Patient-Specific Cardiovascular Computational Modeling: Diversity of Personalization and Challenges. *Journal of cardiovascular translational research, 11*(2), 80–88. https://doi.org/10.1007/s12265-018-9792-2

[51] Crispi, F., Valenzuela-Alcaraz, B., Cruz-Lemini, M., & Gratacós, E. (2013). Ultrasound assessment of fetal cardiac function. *Australasian journal of ultrasound in medicine, 16*(4), 158–167. https://doi.org/10.1002/j.2205-0140.2013.tb00242.x

[52] Pennati, G., & Fumero, R. (2000). Scaling approach to study the changes through the gestation of human fetal cardiac and circulatory behaviors. *Annals of biomedical engineering, 28*(4), 442–452. https://doi.org/10.1114/1.282

[53] Avanzolini, G., Barbini, P., Cappello, A., & Cevese, A. (1985). Time-varying mechanical properties of the left ventricle--a computer simulation. *IEEE transactions on bio-medical engineering, 32*(10), 756–763. https://doi.org/10.1109/TBME.1985.325490

[54] Zhu, S., Luo, L., Yang, B., Li, X., & Wang, X. (2017). Improving hemodynamics of cardiovascular system under a novel intraventricular assist device support via modeling and simulations. *Computer assisted surgery (Abingdon, England), 22*(sup1), 221–231. https://doi.org/10.1080/24699322.2017.1389400

[55] Gallivan, S., Robson, S. C., Chang, T. C., Vaughan, J., & Spencer, J. A. (1993). An investigation of fetal growth using serial ultrasound data. Ultrasound in obstetrics & gynecology : *the official journal of the International Society of Ultrasound in Obstetrics and Gynecology, 3*(2), 109–114. https://doi.org/10.1046/j.1469-0705.1993.03020109.x

[56] Bozkurt S (2019) Mathematical modeling of cardiac function to evaluate clinical cases in adults and children. *PLOS ONE 14*(10): e0224663. https://doi.org/10.1371/journal.pone.0224663

[57] Yellin, E. L., Peskin, C. S., & Frater, R. W. M. (1972). Pulsatile flow across the mitral valve: hydraulic, electronic and digital computer simulation. Paper presented at Unknown conference. ASME72-WA BHF-10.

[58] García-Otero, L., Gómez, O., Rodriguez-López, M., Torres, X., Soveral, I., Sepúlveda-Martínez, Á., Guirado, L., Valenzuela-Alcaraz, B., López, M., Martínez, J. M., Gratacós, E., & Crispi, F. (2020). Nomograms of Fetal Cardiac Dimensions at 18-41 Weeks of Gestation. *Fetal diagnosis and therapy, 47*(5), 387–398. https://doi.org/10.1159/000494838

[59] van Ark, A. E., Molenschot, M. C., Wesseling, M. H., de Vries, W. B., Strengers, J., Adams, A., & Breur, J. (2018). Cardiac Valve Annulus Diameters in Extremely Preterm Infants: A Cross-Sectional Echocardiographic Study. *Neonatology, 114*(3), 198–204. https://doi.org/10.1159/000488387

[60] De Smedt, M. C., Visser, G. H., & Meijboom, E. J. (1987). Fetal cardiac output estimated by Doppler echocardiography during mid- and late gestation. *The American journal of cardiology, 60*(4), 338–342. https://doi.org/10.1016/0002-9149(87)90238-4

[61] Struijk, P. C., Mathews, V. J., Loupas, T., Stewart, P. A., Clark, E. B., Steegers, E. A., & Wladimiroff, J. W. (2008). Blood pressure estimation in the human fetal descending aorta. *Ultrasound in obstetrics & gynecology : the official journal of the International Society of Ultrasound in Obstetrics and Gynecology, 32*(5), 673–681. https://doi.org/10.1002/uog.6137

[62] Surrogate optimization for global minimization of time-consuming objective functions - MATLAB (2021). https://www.mathworks.com/help/gads/surrogateopt.html. Accessed: November 2021

[63] Vaillant, M. C., Chantepie, A., Cheliakine, C., Nashashibi, M., Pottier, J. M., & Laugier, J. (1992). Apport de l'échographie bidimensionnelle dans la prédiction de fermeture spontanée des communications interventriculaires du nourrisson [Contribution of two-dimensional echography in predicting spontaneous closure of interventricular defects in infants]. *Archives des maladies du coeur et des vaisseaux, 85*(5), 597–601.

[64] Chantepie, A., Luksenberg, S., Vaillant, M. C., Pottier, J. M., Magontier, N., Despert, F., & Neville, P. (1999). Evolution des communications interventriculaires membraneuses. Relation avec l'anatomie échocardiographique [Evolution of ventricular septal defects. Relation to echocardiographic anatomy]. *Archives des maladies du coeur et des vaisseaux, 92*(5), 623–628.

[65] Baumgartner, H., Hung, J., Bermejo, J., Chambers, J. B., Evangelista, A., Griffin, B. P., Iung, B., Otto, C. M., Pellikka, P. A., Quiñones, M., American Society of Echocardiography, & European Association of Echocardiography (2009). Echocardiographic assessment of valve stenosis: EAE/ASE recommendations for clinical practice. *Journal of the American Society of Echocardiography : official publication of the American Society of Echocardiography, 22*(1), 1–102. https://doi.org/10.1016/j.echo.2008.11.029

[66] American College of Cardiology/American Heart Association Task Force on Practice Guidelines, Society of Cardiovascular Anesthesiologists, Society for Cardiovascular Angiography and Interventions, Society of Thoracic Surgeons, Bonow, R. O., Carabello, B. A., Kanu, C., de Leon, A. C., Jr, Faxon, D. P., Freed, M. D., Gaasch, W. H., Lytle, B. W., Nishimura, R. A., O'Gara, P. T., O'Rourke, R. A., Otto, C. M., Shah, P. M., Shanewise, J. S., Smith, S. C., Jr, Jacobs, A. K., … Riegel, B. (2006). ACC/AHA 2006 guidelines for the management of patients with valvular heart disease: a report of the American College of Cardiology/American Heart Association Task Force on Practice Guidelines (writing committee to revise the 1998 Guidelines for the Management of Patients With Valvular Heart Disease): developed in collaboration with the Society of Cardiovascular Anesthesiologists: endorsed by the Society for Cardiovascular Angiography and Interventions and the Society of Thoracic Surgeons. *Circulation, 114*(5), e84–e231. https://doi.org/10.1161/CIRCULATIONAHA.106.176857

[67] Scholz, T., Reinking B. E. (2018). '55 - Congenital Heart Disease', Editor(s): Christine A. Gleason, Sandra E. Juul, *Avery's Diseases of the Newborn (Tenth Edition)*, Elsevier, pp 801-827.e2, https://doi.org/10.1016/B978-0-323-40139-5.00055-3.

[68] Castor, S., Fouron, J. C., Teyssier, G., Sonnesson, S. E., Chartrand, C., & Skoll, A. (1996). Assessment of fetal pulmonic stenosis by ultrasonography. *Journal of the American Society of Echocardiography : official publication of the American Society of Echocardiography, 9*(6), 805–813. https://doi.org/10.1016/s0894-7317(96)90471-x

[69] Dakkak, W., & Oliver, T. I. (2021). Ventricular Septal Defect. In *StatPearls*. StatPearls Publishing. Accessed: December 2021

[70] Johnson, P., Maxwell, D. J., Tynan, M. J., & Allan, L. D. (2000). Intracardiac pressures in the human fetus. *Heart (British Cardiac Society), 84*(1), 59–63. https://doi.org/10.1136/heart.84.1.59

[71] Chao, R. C., Ho, E. S. C., & Hsieh, K. S. (1994). Fluctuations of interventricular shunting in a fetus with an isolated ventricular septal defect. *American heart journal, 127*(4), 955-958.

[72] Wiputra, H., Chen, C. K., Talbi, E., Lim, G. L., Soomar, S. M., Biswas, A., Mattar, C., Bark, D., Leo, H. L., & Yap, C. H. (2018). Human fetal hearts with tetralogy of Fallot have altered fluid dynamics and forces. *American journal of physiology. Heart and circulatory physiology, 315*(6), H1649–H1659. https://doi.org/10.1152/ajpheart.00235.2018

[73] Kannan B. R. (2008). Tetralogy of Fallot. *Annals of pediatric cardiology, 1(*2), 135–138. https://doi.org/10.4103/0974-2069.43880

[74] AEPD - Agencia Española de Protección de Datos. (2019). Guía para pacientes y usuarios de la Sanidad.

[75] UNE-EN 61157:2007/A1:2013 (Ratificada). AENOR. (2013). https://www.aenor.com/normas-y-libros/buscador-de-normas/une?c=N0051008. Accessed: December 2021.

[76] UNE-EN 61266:1996. AENOR (1996). https://www.aenor.cat/normas-y-libros/buscador-de-normas/une/?c=N0012943. Accessed: December 2021.

[77] ISO 9001 Certification. AENOR. (2015). https://www.en.aenor.com/certificacion/calidad/iso-9001. Accessed: December 2021.

[78] ISO 13379-1:2012(en), Condition monitoring and diagnostics of machines — Data interpretation and diagnostics techniques — Part 1: General guidelines. ISO. (2012). https://www.iso.org/obp/ui/#iso:std:iso:13379:-1:ed-1:v1:en. Accessed: December 2021.

APPENDIX

Appendix A – Parametric analysis in healthy conditions

Peripheral resistances and compliances of pulmonary and systemic vascular beds

Here, the resulting plots of the variation of the systemic circulation vascular bed peripheral compliance (C_s), the pulmonary vascular bed peripheral resistance (R_{lungs}), and the systemic vascular bed peripheral resistance (R_s) are presented.

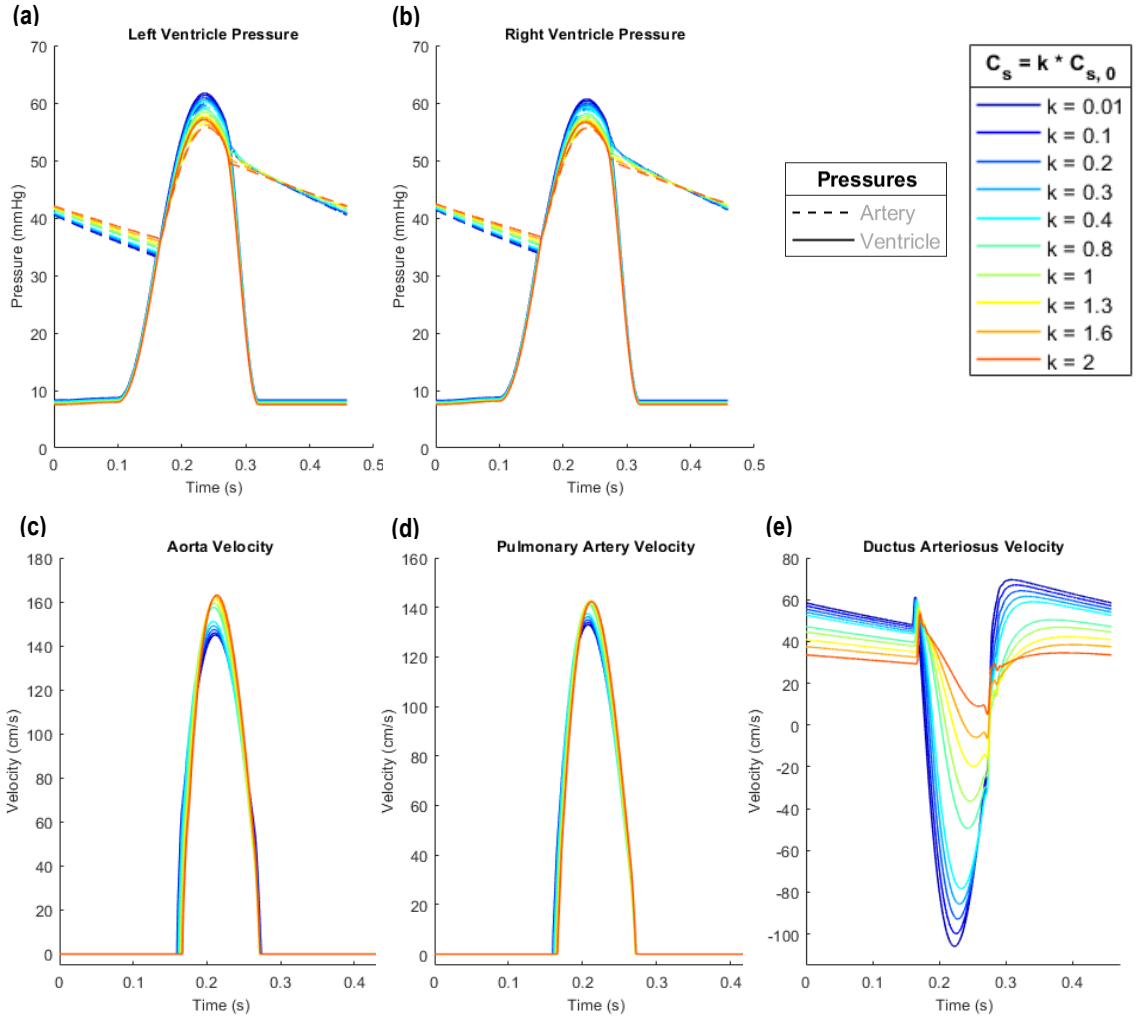

Figure A1. Model-based waveforms resulting from the parametric study on the variation of the peripheral compliance of the systemic circulation vascular bed (C_s): a) left ventricle and aorta pressure; b) right ventricle and pulmonary artery pressure; c) aorta velocity; d) pulmonary artery velocity; e) DA velocity

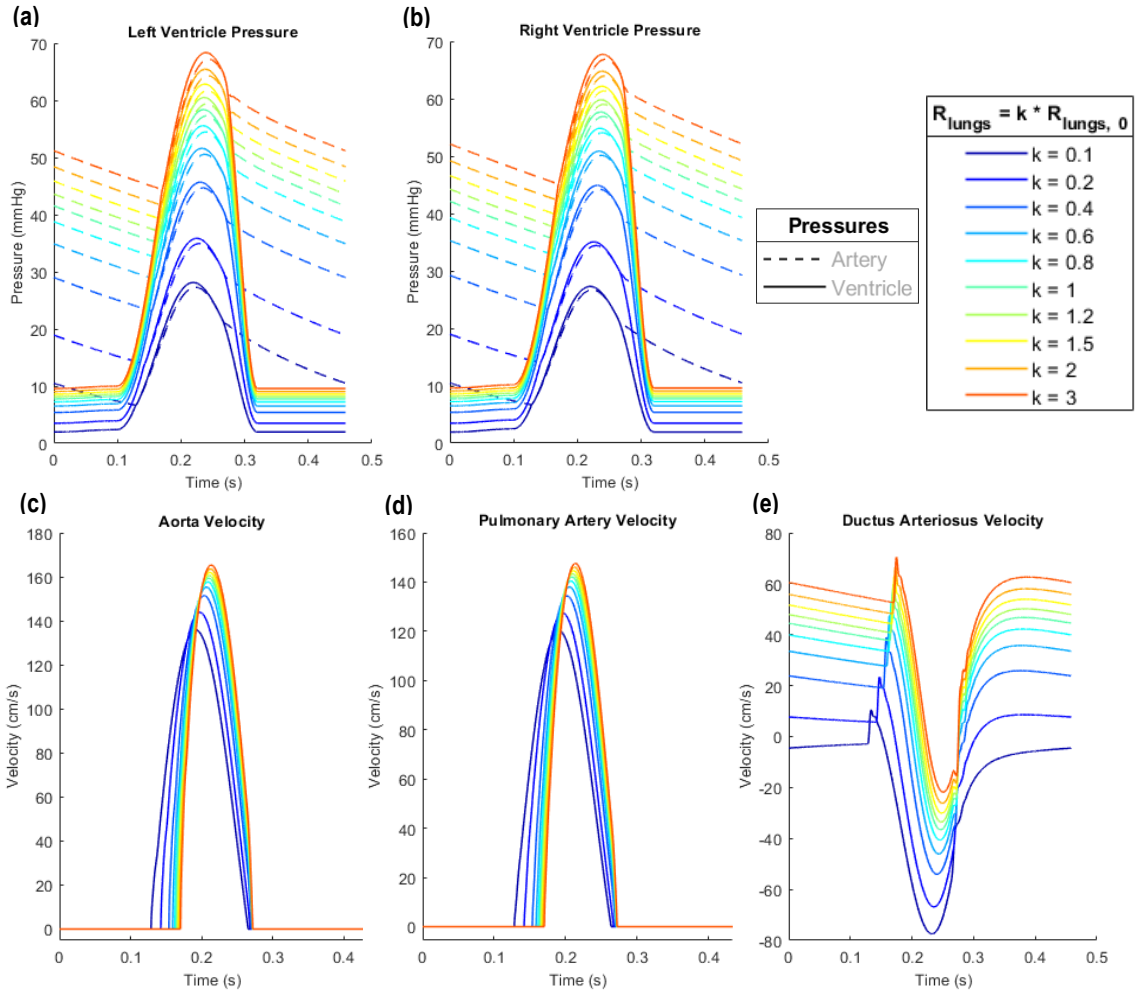

Figure A2. Model-based waveforms resulting from the parametric study on the variation of the peripheral resistance of the pulmonary circulation vascular bed (R_{lungs}): a) left ventricle and aorta pressure; b) right ventricle and pulmonary artery pressure; c) aorta velocity; d) pulmonary artery velocity; e) DA velocity

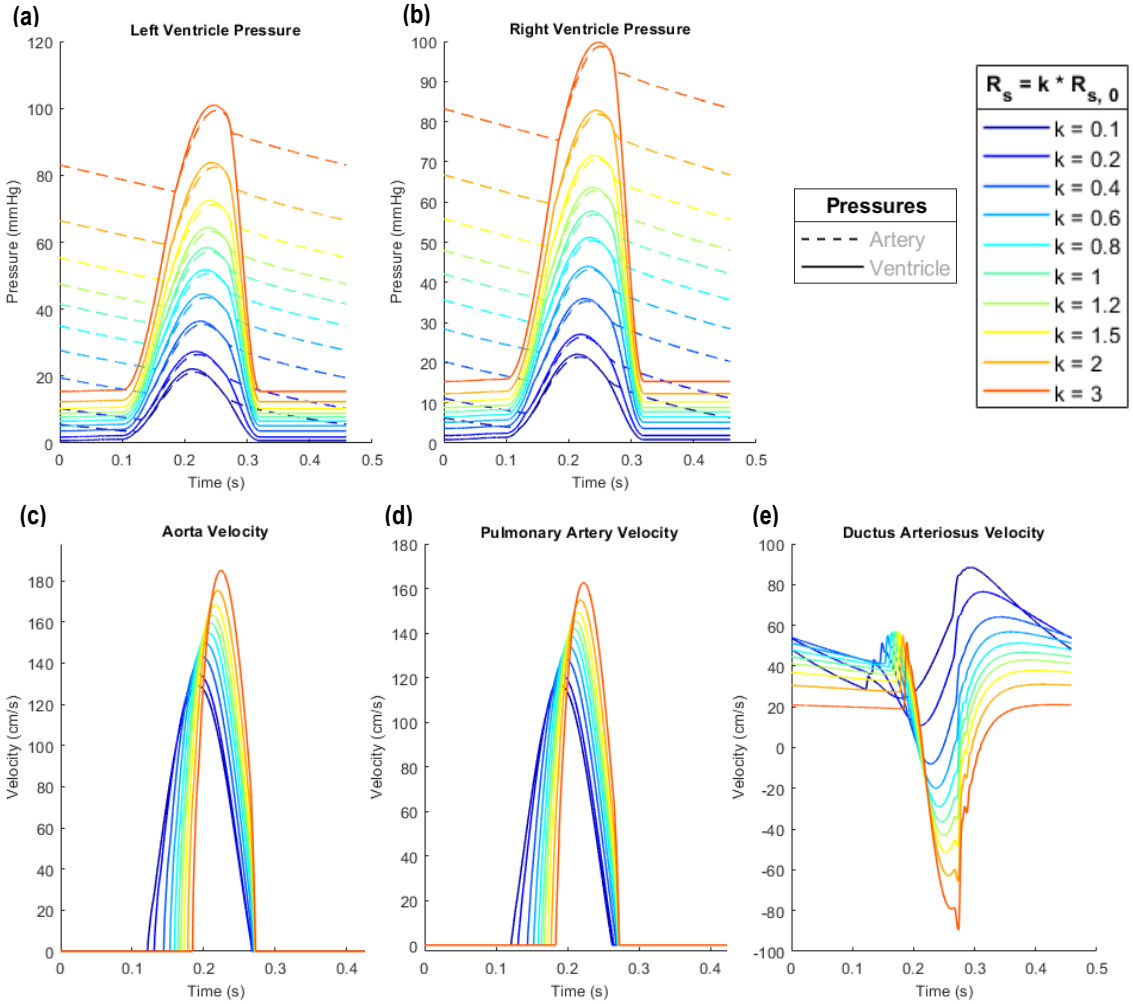

Figure A3. Model-based waveforms resulting from the parametric study on the variation of the peripheral resistance of the systemic circulation vascular bed (R_s): a) left ventricle and aorta pressure; b) right ventricle and pulmonary artery pressure; c) aorta velocity; d) pulmonary artery velocity; e) DA velocity

Appendix B – Parametric analysis in healthy conditions

Ventricular activation timings

Here, the resulting plots of the variation of the ventricular activation timings (duration of the ventricular contraction and delay between atrial and ventricular contraction) are presented. First, the two resulting plots of the elastance curve are shown and then, there are the model-based pressure and velocity waveforms.

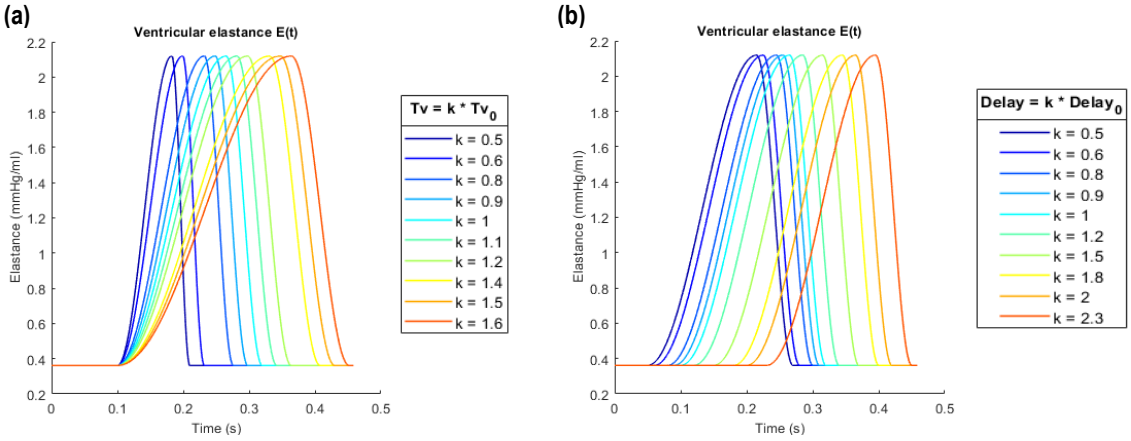

Figure B1. Model-based elastance waveform resulting from the parametric study on the variation of: a) ventricular contraction duration (T_v); b) delay between atrial and ventricular contraction ($delay$)

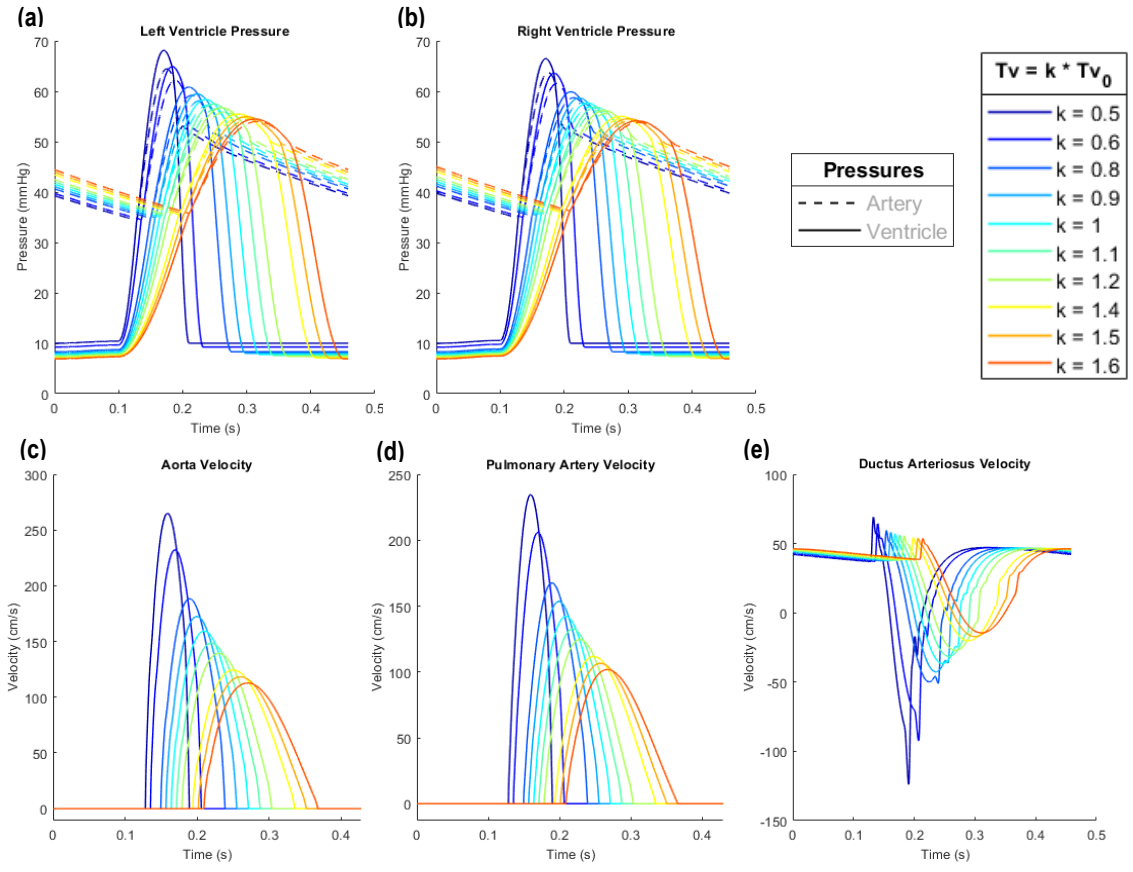

Figure B2. Model-based waveforms resulting from the parametric study on the variation of the ventricular contraction duration (T_v): a) left ventricle and aorta pressure; b) right ventricle and pulmonary artery pressure; c) aorta velocity; d) pulmonary artery velocity; e) DA velocity

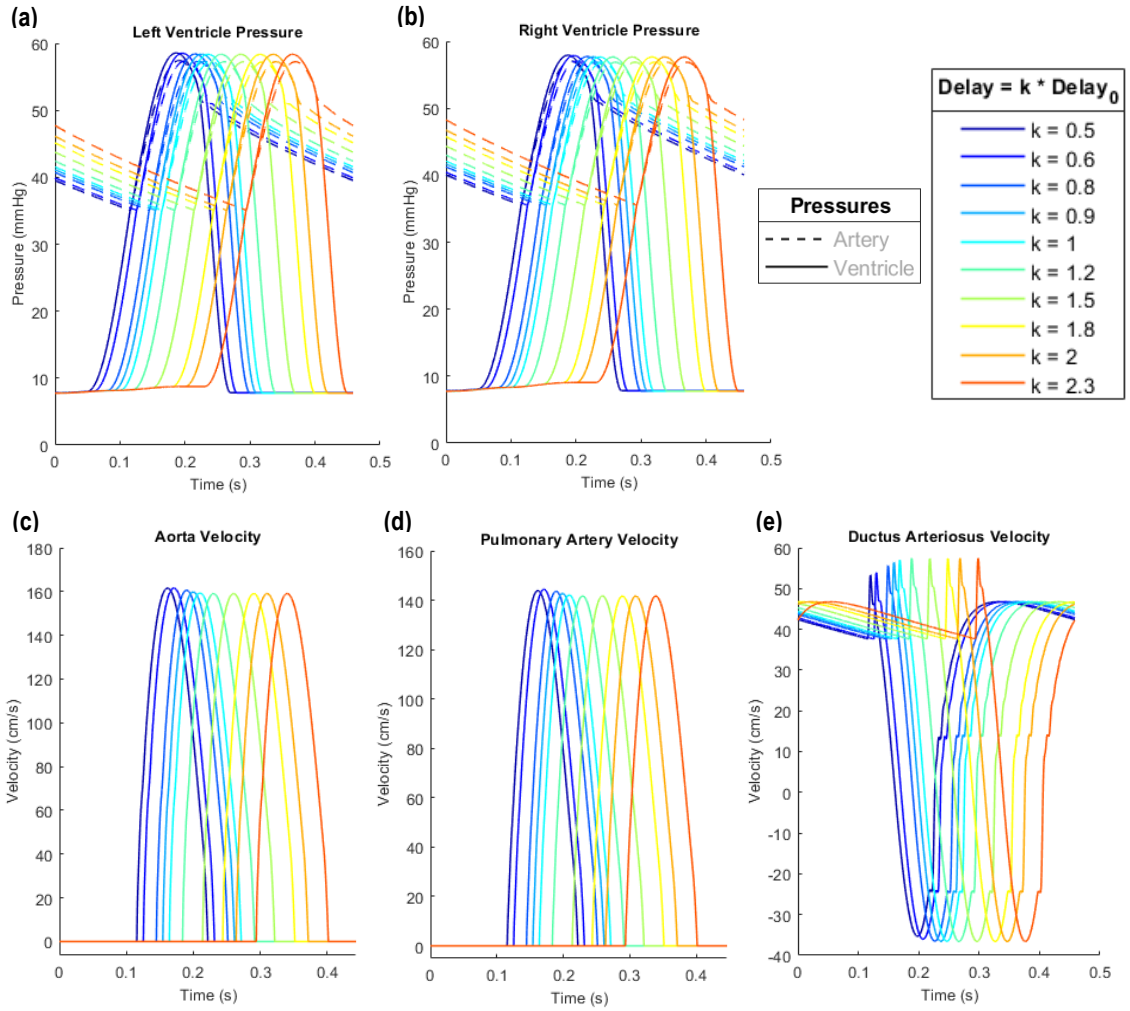

Figure B3. Model-based waveforms resulting from the parametric study on the variation of the delay between atrial and ventricular contraction ($delay$): a) left ventricle and aorta pressure; b) right ventricle and pulmonary artery pressure; c) aorta velocity; d) pulmonary artery velocity; e) DA velocity

Appendix C – Parametric analysis in healthy conditions

Diameters of mitral and tricuspid valves

Here, the resulting plots of the variation of the tricuspid valve diameter are presented.

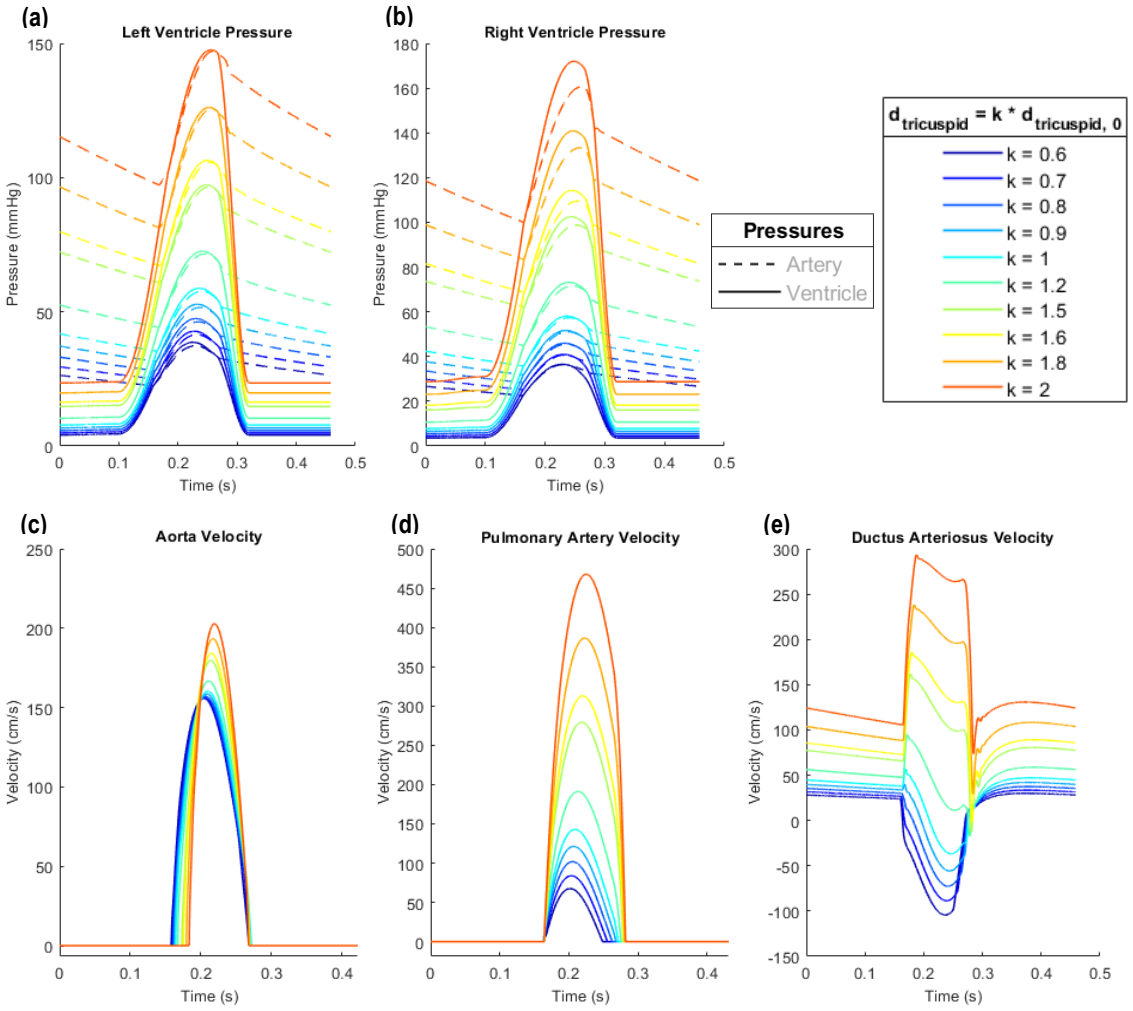

Figure C1. Model-based waveforms resulting from the parametric study on the variation of the tricuspid valve diameter: a) left ventricle and aorta pressure; b) right ventricle and pulmonary artery pressure; c) aorta velocity; d) pulmonary artery velocity; e) DA velocity

Appendix D – Calibration of the simplified model of the fetal heart in healthy conditions

In this section, the resulting plots of blood flow, velocity, pressure and volume of different segments of the fetal circulatory system are presented, after having performed the calibration of the fetal heart 0D lumped model. First, there is the blood flow of left and right ventricles *(Fig.D1)*, then, the pressure-volume relationship of both ventricles is shown *(Fig.D2)* and, finally, the velocity profiles of both aortic and pulmonary valves *(Fig.D3)* and pulmonary circulatory system *(Fig.D4)* are depicted.

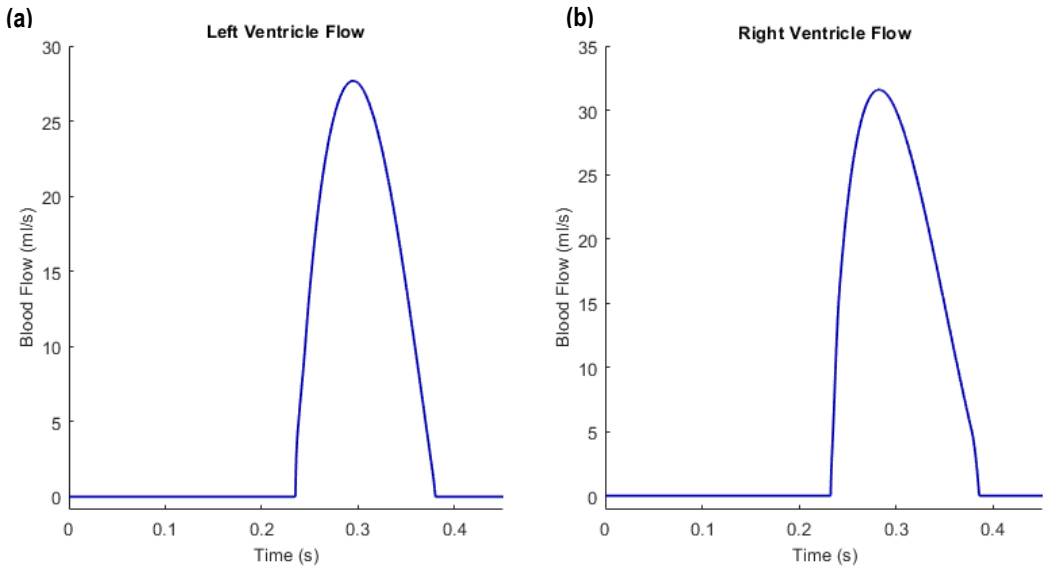

Figure D1. Model-based blood flow in a) left and b) right ventricles, after calibration of the fetal heart 0D lumped model

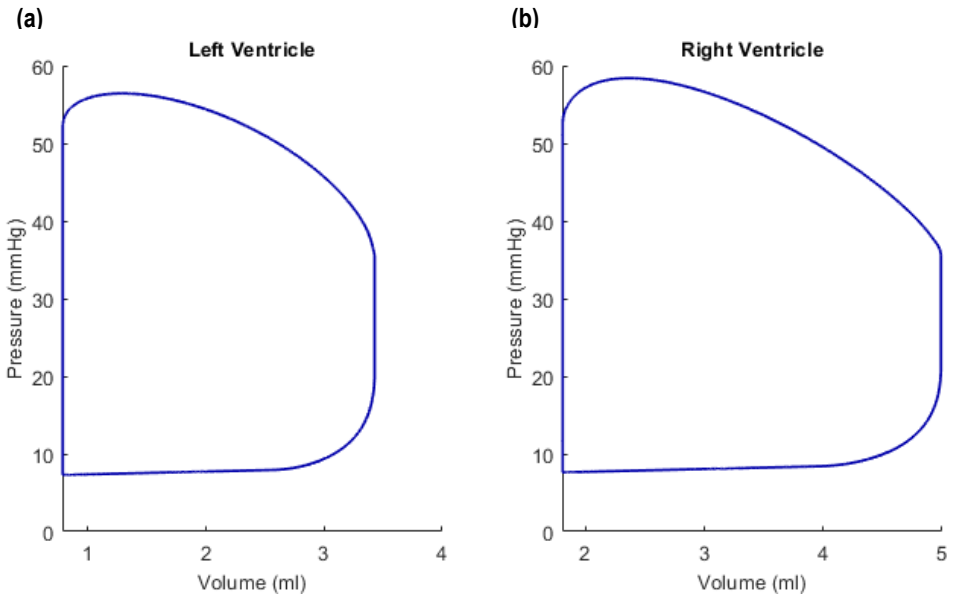

*Figure D2.*Model-based pressure-volume relationship of a) left and b) right ventricles, after calibration of the fetal heart 0D lumped model

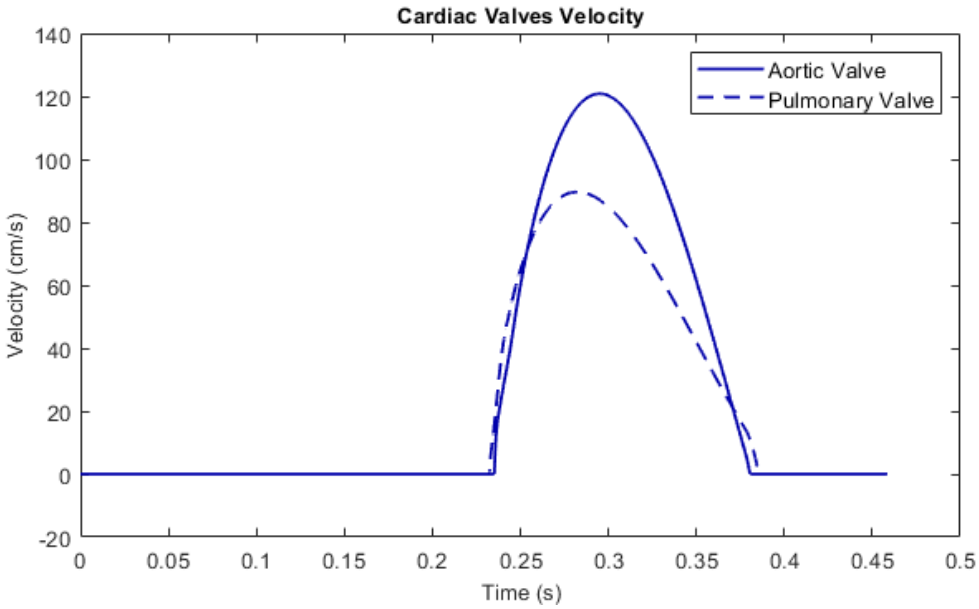

Figure D3. Model-based velocity profile of aortic (solid line) and pulmonary (dashed line) valves, after calibration of the fetal heart 0D lumped model

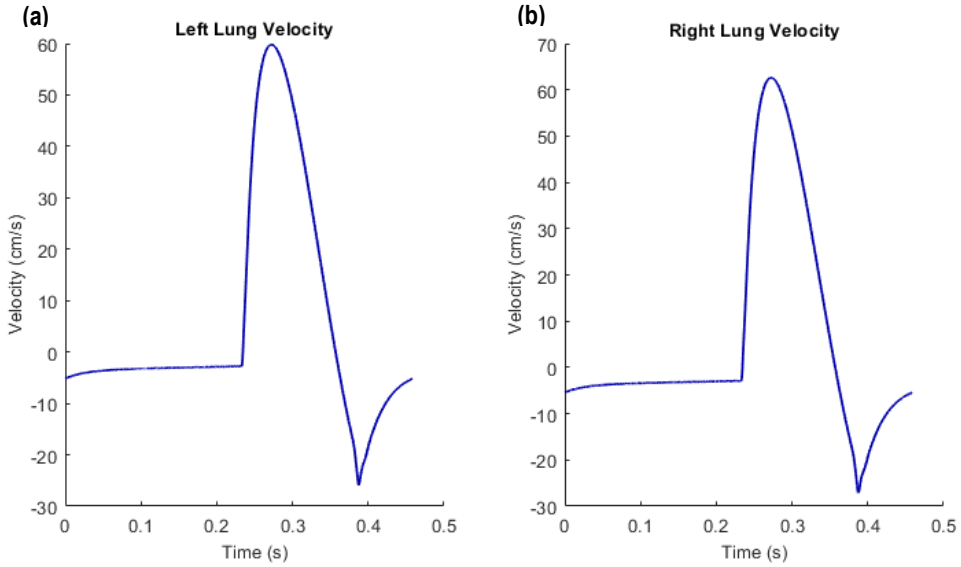

Figure D4. Model-based blood velocity profiles of the pulmonary circulatory system: a) left and b) right lungs, after calibration of the fetal heart 0D lumped model